



National Defence
Research and
Development Branch

Défense nationale
Bureau de recherche
et développement

**PROPAGATION-LOSS MEASUREMENTS AND
MODELLING FOR TOPOGRAPHICALLY
SMOOTH AND ROUGH SEABEDS.**

Philip R. Staal - Francine Desharnais

June 1989

Approved by R. S. Walker
A/D/Underwater Acoustics Division

Distribution Approved by


A/D/UAD

TECHNICAL MEMORANDUM 89/214

**Defence
Research
Establishment
Atlantic**



**Centre de
Recherches pour la
Défense
Atlantique**

Canada

ABSTRACT

Acoustic propagation loss data were obtained along two radial tracks from a receiving array at a site on the Scotian Shelf. One track was over a smooth seabed and the other over a rough seabed. The features of the propagation loss data for the two seabed types have been analyzed and compared. At-sea measurements show that fluctuations in the propagation loss data are correlated with water-depth variations for the case of the rough seabed. Two different propagation-loss modelling programs are used in an attempt to explain the acoustic features observed over the two seabeds. The majority of the modelled results were obtained with PROLOS, a DREA-developed range-dependent normal-mode program. The results of a ray-trace propagation-loss model (GRASS) are also compared with the measured data. The ray-trace model provides insight on which acoustic transmission paths are most important, while PROLOS is able to model the propagation-loss over both the smooth and rough seabeds surprisingly well.

RÉSUMÉ

Des données de propagation acoustique ont été prises le long de deux trajectoires orientées vers une série de senseurs situés sur le plateau continental près de la Nouvelle-Ecosse. Le fond marin, relativement plat le long d'une des trajectoires, est de profondeur très variable dans l'autre direction, ce qui permet d'analyser et de comparer les différentes caractéristiques de la propagation acoustique pour ces deux fonds marins. Les données collectées en mer montrent que les fluctuations notées dans la propagation acoustique sont reliées aux variations dans l'épaisseur de la colonne d'eau, pour le cas où cette dernière est très variable. Deux modèles géo-acoustiques différents ont été utilisés pour tenter d'expliquer les caractéristiques de la propagation acoustique pour les deux cas. La majorité des résultats ont été obtenus avec PROLOS, un modèle du CRDA utilisant la théorie des modes normaux et permettant la variation du sol marin avec la distance. GRASS, un autre modèle basé sur la méthode des rayons (théorie de l'acoustique géométrique), a aussi produit certains résultats qui ont été comparés avec les données expérimentales. Ce dernier modèle a démontré quelles trajectoires acoustiques sont préférentielles, alors que PROLOS a permis de prédire étonnamment bien les pertes acoustiques au-dessus des deux types différents de fonds marins.

TABLE OF CONTENTS

Section	Page
ABSTRACT	ii
RÉSUMÉ	ii
TABLE OF CONTENTS	iii
LIST OF FIGURES	iv
LIST OF TABLES	v
1. INTRODUCTION	1
2. EXPERIMENTAL DATA	1
2.1. SMOOTH SEABED	5
2.2. ROUGH SEABED	6
2.2.1. Propagation loss for a hydrophone depth of 75.6 m	7
2.2.2. Propagation loss for a hydrophone depth of 62.1 m	10
2.3. COMPARISON OF LOSS FOR SMOOTH AND ROUGH SEABEDS	11
3. MODELLING AND COMPARISON	13
3.1. SMOOTH SEABED	13
3.1.1. PROLOS	13
3.1.1.1. PROLOS with a two-layer seabed	14
3.1.1.2. PROLOS with a three-layer seabed	16
3.1.3. Comparison between the experimental results (over the smooth seabed) and the modelled results	17
3.2. ROUGH SEABED	17
3.2.1. GRASS	19
3.2.2. PROLOS	20
3.2.2.1. PROLOS results for a hydrophone depth of 75.6 m (near the seabed)	21
3.2.2.2. PROLOS results for a hydrophone depth of 62.1 m (in the sound channel)	24
3.2.3. Comparison between the experimental results (over the rough seabed) and the modelled results.	26
4. CONCLUSIONS	28
REFERENCES	30

LIST OF FIGURES

Figure	Page
1. Typical deployment of the Hydra array on the seabed.	2
2. XBTs and seabed profile for the smooth seabed.	3
3. Average experimental propagation loss (from 3 to 645 Hz) to the deepest hydrophone (75.6 m) as a function of range. Seabed depth and bedrock depth as a function of distance from the receiving hydrophone array for the smooth seabed are also shown.....	4
4. Third-octave measurements of propagation loss to the deepest hydrophone (75.6 m) versus frequency for various ranges over the smooth seabed.	6
5. XBTs and seabed profile for the rough seabed.	7
6. Frequency-averaged experimental propagation loss (with spherical spreading removed) to the deepest hydrophone as a function of range. Seabed depth and bedrock depth as a function of distance from the receiving hydrophone array for the rough seabed are also shown.	8
7. Third-octave measurements of propagation loss to the deepest hydrophone (75.6 m) versus frequency for various ranges over the rough seabed.	9
8. Frequency-averaged experimental propagation loss (with spherical spreading removed) to the 62.1 m deep hydrophone as a function of range. Seabed depth and bedrock depth as a function of distance from the receiving hydrophone array for the rough seabed are also shown.	10
9. Comparison of experimental propagation loss versus range for the rough and smooth seabeds; for frequencies: 25 Hz, 102 Hz and 406 Hz.	12
10. Comparison at 40 Hz, 102 Hz and 406 Hz of experimental and theoretical propagation loss to the deepest hydrophone (75.6 m) versus range over the smooth seabed. The model used is PROLOS with a two-layer seabed, and the results for both coherent and incoherent mode addition are shown.	15
11. Approximate map of the two parts of track SS over the smooth seabed relative to the Hydra array.	16
12. Comparison at 40 Hz, 102 Hz and 406 Hz of experimental and theoretical propagation loss to the deepest hydrophone (75.6 m) versus range over the smooth seabed. The model used is PROLOS with a three-layer seabed, and the results for both coherent and incoherent mode addition are shown.	18
13. Seabed depth as a function of distance from the receiving hydrophone array for the rough seabed. A 2.5 degree (off horizontal) ray-path and a 7.5 degree ray-path from the deepest hydrophone (75.6 m) are superimposed on these bathymetric plots.	20
14. Comparison of experimental and theoretical propagation loss to the deepest hydrophone (75.6 m) versus range over the rough seabed. This comparison is shown at three frequencies: 25 Hz, 161 Hz and 645 Hz. The model used is PROLOS with a three-layer seabed, and the results for both coherent and incoherent mode addition are shown. The water depth along track RS is shown at the bottom.	23

LIST OF FIGURES (cont'd)

Figure	Page
15. Frequency-averaged theoretical propagation loss (with spherical spreading removed) to the deepest hydrophone (75.6 m) as a function of range. Seabed depth and bedrock depth as a function of distance from the receiving hydrophone array for the rough seabed are also shown.	24
16. Comparison of experimental and theoretical propagation loss to the 62.1 m deep hydrophone versus range over the rough seabed. This comparison is shown at three frequencies: 25 Hz, 161 Hz and 645 Hz. The model used is PROLOS with a three-layer seabed, and the results for both coherent and incoherent mode addition are shown. The water depth along track RS is shown at the bottom.	25
17. Comparison of experimental and theoretical propagation loss to the deepest hydrophone (75.6 m) versus range over the rough seabed. This comparison is shown at three frequencies: 25 Hz, 161 Hz and 645 Hz. The model used is PROLOS with a three-layer seabed, and the results for both coherent and incoherent mode addition are shown. The water depth along track RS is shown at the bottom. This figure is identical to Fig. 14, except that the water layer was isospeed in the model.	27

LIST OF TABLES

Table	Page
I. Water depth, sediment thickness, and sound-speed profiles input to PROLOS for the case of propagation over the smooth seabed.	13
II. Two-layer seabed parameters for PROLOS.	14
III. Three-layer seabed parameters for PROLOS.	16
IV. Reflection loss versus grazing angle for sand.	19
V. Water depth, sediment thickness, and sound-speed profiles input to PROLOS for the case of propagation over the rough seabed.	22

1. INTRODUCTION

The propagation of sound in shallow water is strongly influenced by the seabed. In fact, the water depth, sound-speed profile, and the seabed's composition and roughness are of primary importance in determining acoustic propagation conditions in shallow water. Starting in 1980, the Shallow Water Acoustics Group at DREA has studied the influence of a nearly flat sand seabed [Ellis and Chapman, 1980], a nearly flat chalk seabed [Staal, 1983], and later a nearly flat granite seabed [Staal, Chapman and Zakarauskas, 1986]. The Group has also studied sea-surface roughness [Chapman, 1980] and seabed roughness [Staal, Chapman and Zakarauskas, 1986]. This Technical Memorandum describes the Group's first study of acoustic propagation over a seabed with highly variable water depth (i.e. a "topographically rough" seabed), a type of seabed that has been assumed to be very difficult to model.

Other researchers have studied acoustic propagation through waters of variable depth, but normally in the form of a simple monotonically sloping seabed (for example: [Akal and Jensen, 1986]). Conversely, reported herein is the analysis of an experiment in an area of the Scotian Shelf where the water depth varies between about 90 m and 210 m on a scale of a few kilometres in range.

The array location was selected to be near a seabed-type transition - on the boundary between a topographically smooth and a topographically rough seabed - so as to permit a comparison of the effect of the seabed type upon sound propagation [Staal, 1983]. Conditions in the water column were similar over the two seabed types. In this memorandum, we examine some of the implied effects of topographic roughness on propagation loss.

In this memorandum, there are two main sections: Section 2, that describes the experimental data, and Section 3, that describes the modelled results and their comparison with the experimental data of Section 2. In each of these main sections, the results are discussed first for the smooth seabed, and then for the rough seabed. Conclusions are presented in Section 4.

2. EXPERIMENTAL DATA

The chosen experimental area is on the edge of a shallow-water sand bank on the Scotian Shelf. The array of hydrophones (Hydra, described in [Staal, Hughes and Olsen, 1981]; [Staal, 1987]) was deployed from the research vessel CFAV QUEST, at the boundary between topographically smooth and topographically rough seabed regions. Figure 1 shows a typical deployment of the Hydra array on the seabed, and the radio data link to the vessel. For the present study, the array consisted of 10 hydrophones spaced vertically in the water column. We chose to study the propagation loss for only two of the receiver depths: at 75.6 m which was the depth of the deepest hydrophone (almost at the seabed), and at 62.1 m, which was near the centre of a sound channel observed for one of the tracks.

A second vessel, HMCS CORMORANT, travelled along two radial tracks from the Hydra array: one direction over the smooth seabed (track "SS") and one direction over the rough seabed (track "RS"). This latter track has a "topographic RMS roughness" of ≈ 60 m about a mean depth of ≈ 150 m, with predominant spatial wavelengths from about 5 to 15 km. For the acoustic frequencies considered in this memorandum, this topographic roughness consists of features that block propagation, and act as sloping bottoms. Features that act as scatterers, are not considered here. For more information on the properties of seabed roughness, see [Berkson and Matthews, 1983]. CORMORANT deployed 0.454 kg (1 lb) explosive sound sources at horizontal intervals of about 3 km. The charges were set to detonate at a depth of 46 m (150 ft). The source depth was controlled by suspending the charges from floats by measured lengths of string. The actual detonation depths were inferred from the bubble period measured by cepstral analysis of the pressure versus time signature for each shot [Hughes, 1981].

Sound-speed profiles were derived from expendable bathy-thermograph (XBT) records obtained by CORMORANT along the two tracks throughout the experiments. The water depth profile along each track was read from the depth contours on a surficial geology map of the Scotian Shelf (published by the Canadian Hydrographic Service). The thickness of the upper layer of sediment was estimated by interpolation from a sediment-thickness overlay produced for the map [King, Nadeau, Maass and King, 1985].

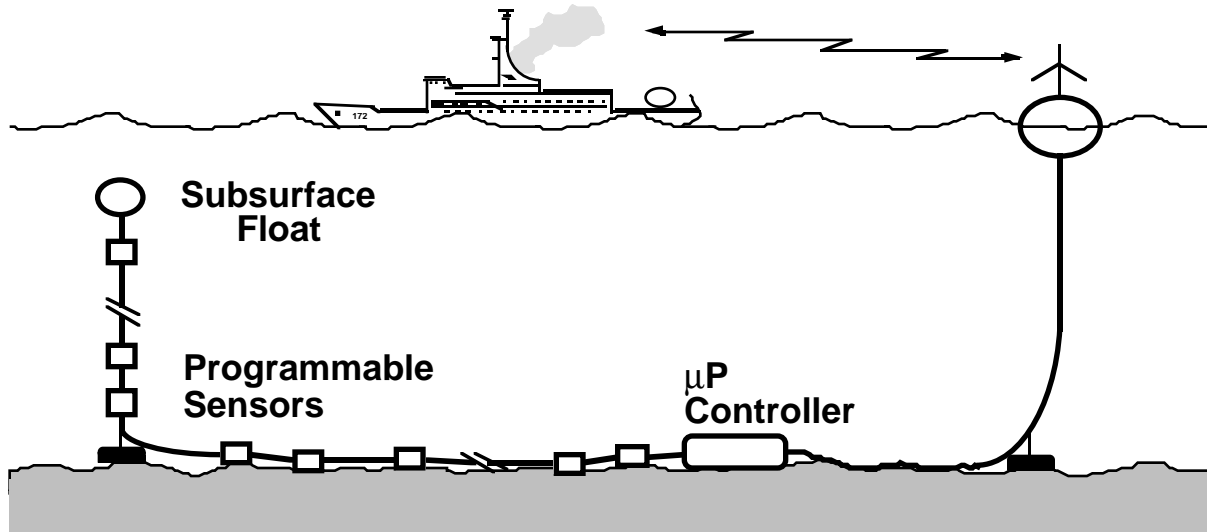


Fig. 1. Typical deployment of the Hydra array on the seabed.

The pressure signals from the explosive sound sources were converted to voltages at the Hydra array hydrophones. The voltage from each hydrophone was amplified, filtered and digitized within each hydrophone container, then transmitted along cables to a surface buoy, and transmitted by radio to the vessel QUEST. On QUEST, the digital signals were recorded on 9-track computer tapes. For each ship track, the data on these tapes were analyzed in order to calculate and plot the acoustic propagation loss (averaged in one-third octave frequency bands) as a function of range, for both of the hydrophone depths considered in this memorandum.

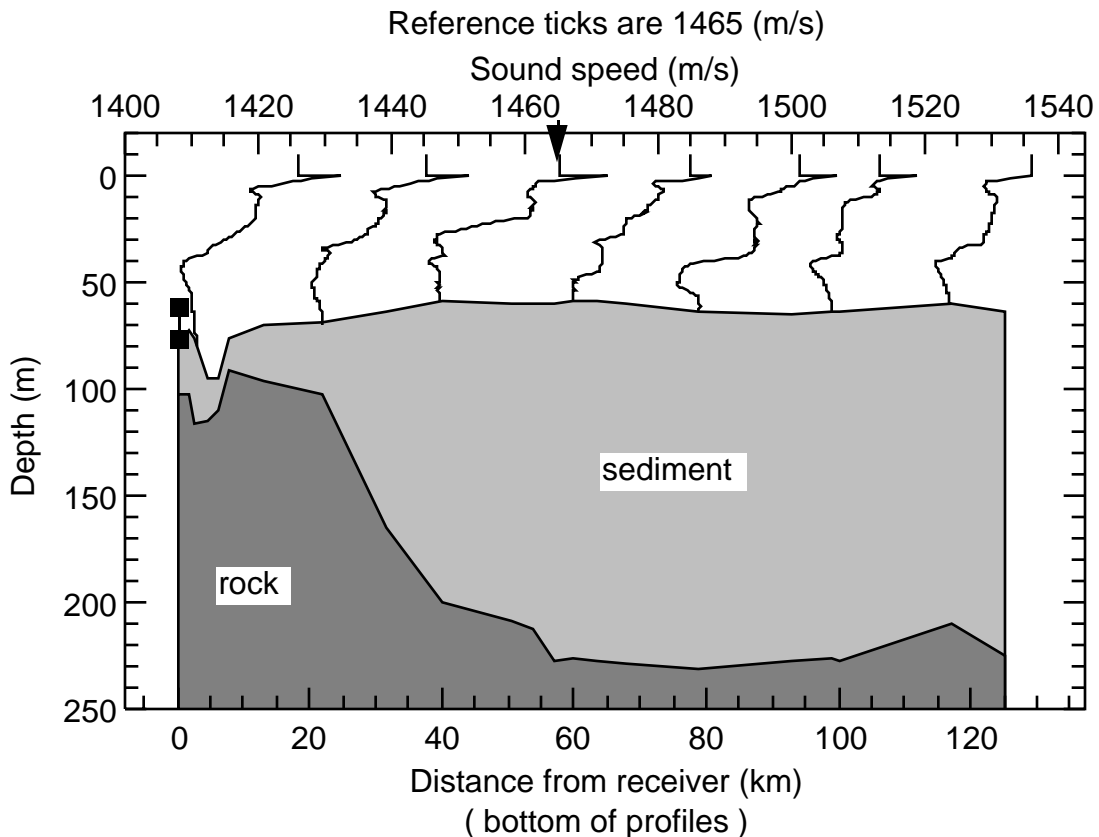


Fig. 2. Seabed depth and bedrock depth as a function of distance from the receiving hydrophone array for the smooth seabed. The two hydrophones used in this study are shown as ■ symbols. Sound-speed data from XBTs are also shown, with their distance from the array indicated by the location of their bottom data points. A reference tick is drawn at the top of each sound-speed trace to indicate 1465 m/s.

The following method was used to calculate the propagation loss: the pressure data from each explosion were discrete Fourier transformed, and the powers in the resulting frequency bins were grouped and averaged to form one-third octave frequency bands of received pressure spectrum level. One-third octave noise estimates were similarly formed from the ambient noise at times just before each explosion. These noise estimates were subtracted from the received pressure spectrum levels to produce noise-corrected pressure spectrum levels. Only one-third octave levels with at least 3 dB signal to noise ratio were used subsequently. Source levels were obtained by scaling the spectrum levels for a 0.454 kg (1 lb) charge exploded at 92.9 m depth. The scaling method used was that described in [Hughes, 1981]. The propagation loss was then taken to be the difference between the source level and the noise-corrected received level for each one-third octave frequency band.

As well as plotting propagation loss versus range, we plotted propagation loss versus frequency, at several ranges. As with the loss-versus-range plots, we plotted the loss-versus-frequency data for the 75.6 m hydrophone depth for track SS and for both 75.6 and 62.1 m depths for track RS.

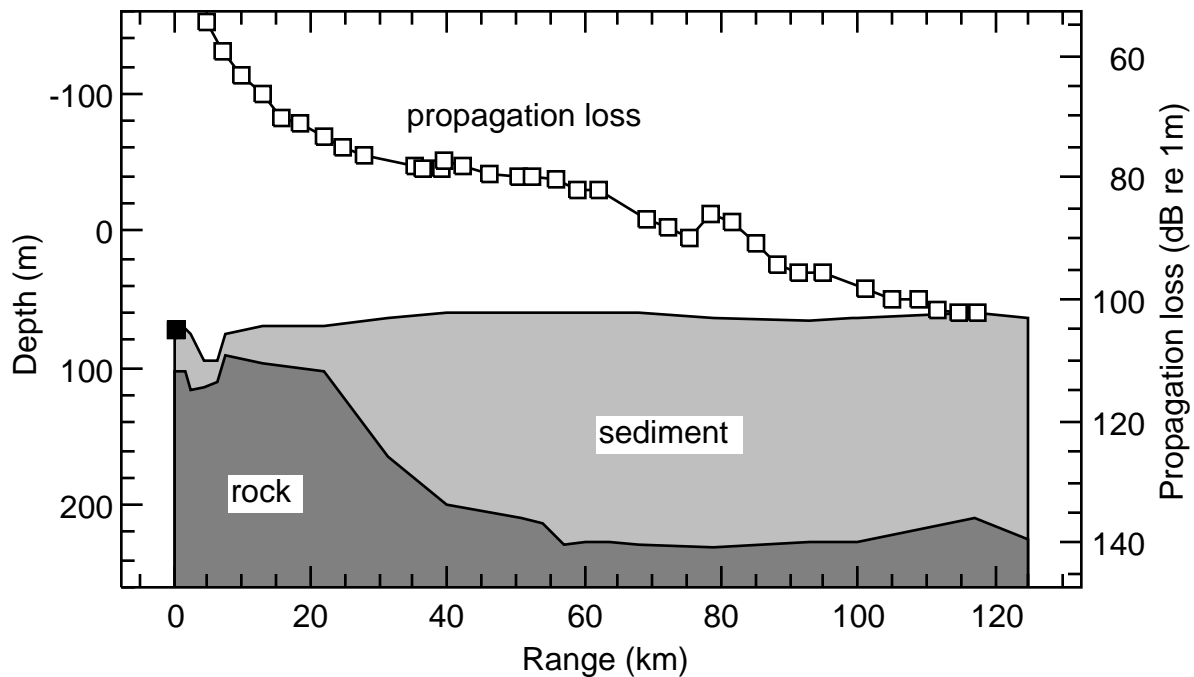


Fig. 3. Average experimental propagation loss (from 3 to 645 Hz) to the deepest hydrophone (75.6 m, marked with ■ symbol) as a function of range. Seabed depth and bedrock depth as a function of distance from the receiving hydrophone array for the smooth seabed are also shown.

2.1. SMOOTH SEABED

Figure 2 shows seabed depth and bedrock depth as a function of distance from the receiving hydrophone array for the smooth seabed. The two hydrophones used in this study are shown as ■ symbols. Sound-speed data from XBTs are also shown, with their distance from the array indicated by the location of their bottom data points. As shown in Fig. 2, the seabed is fairly flat along track SS, but the thickness of the layer of sediment varies from a few metres to more than 160 metres. Data are sparse on the sediment-thickness map, so these numbers may not be entirely accurate. The sound-speed profiles along the track SS were such as to cause a general downward refraction of the sound energy. One thus expects strong acoustic interaction with the seabed.

For track SS we consider only data from the deepest hydrophone: at 75.6 m depth. In Fig. 3, the general features of the propagation loss-versus-range along the track are shown. "Frequency-averaged" propagation loss to the deepest hydrophone is shown as a function of range. The seabed depth and bedrock depth as a function of distance from the receiving hydrophone array for the smooth seabed are also shown. The "frequency average" is defined as the arithmetic mean of the propagation loss, in decibels, of the 1/3 octave bands centred on 3.2, 6.4, 10.1, 16.0, 25.4, 40.3, 64.0, 101.6, 161.3, 256.0, 406.4, and 645.1 Hz.

There is no evident variation in the propagation loss (either for the frequency-averaged data or for the 1/3 octave band data) corresponding to changes in the water depth. The seabed is quite flat though, so one should not expect to see much change. Neither is there an obvious correlation between the propagation loss and the sediment thickness. We were expecting such a correlation, especially at short ranges where the bedrock was closer to the seabed surface. It had been conjectured that the interaction of sound with the bedrock might lead to a noticeable change in the propagation loss. Such is clearly not the case.

Analyzing propagation loss as a function of frequency, we obtain the curves shown in Fig. 4 for five ranges. At the 2.1 km range, the acoustic propagation loss increases with increasing frequency throughout the frequency domain. At longer ranges, however, there is a maximum in the acoustic propagation loss with greatest loss in the region of 5 to 10 Hz. Propagation loss below about 10 Hz is expected to increase due to modal cutoff¹ for the depth of water along track SS. At the two longest ranges (63.1 and 111.5 km), the acoustic propagation loss appears to be abnormally high below 40 Hz. Data for these two ranges were collected during the second part of track SS. It is speculated that the sound for the two greatest ranges must have travelled over a significantly different seabed near the Hydra array than did the sound from the shorter range sources. We suspect that for the second part of track SS, for the two longest ranges illustrated, thinner sediment near the Hydra array may have led to increased propagation loss below 40 Hz.

¹ The mode cutoff frequency is the frequency below which acoustic energy is not effectively trapped in the shallow-water duct [Urick, 1983].

Another interesting feature of the data in Fig. 4 is the reduction in propagation loss at frequencies of about 5 Hz and below. This feature seems to provide evidence of compressional, shear or interface waves propagating in the bottom layers, since the water layer is too thin to carry such long wavelengths by itself (modal cutoff is approximately 10 Hz) [Akal and Jensen, 1986].

2.2. ROUGH SEABED

Figure 5 illustrates the bottom topography and sound velocity structure for track RS. We can see in Fig. 5 that the seabed is topographically very rough. The sediment distribution is also quite complex, and the sediment is generally thinner than for track SS. The sediment-layer thickness varies from about 20 to about 40 metres. Seismic-survey data used for producing the sediment-thickness map are more extensive over the rough seabed area, and thus we are able to obtain greater accuracy in estimating sediment thickness for track RS. The sound-speed profiles here are indicative of predominantly downward refracting conditions for the shallower portions of track RS, indicating strong acoustic interaction with the seabed in these shallow areas. In the deeper valleys however, a sound channel is formed; this is expected to reduce the interaction of sound with the seabed over the deeper portions of the track.

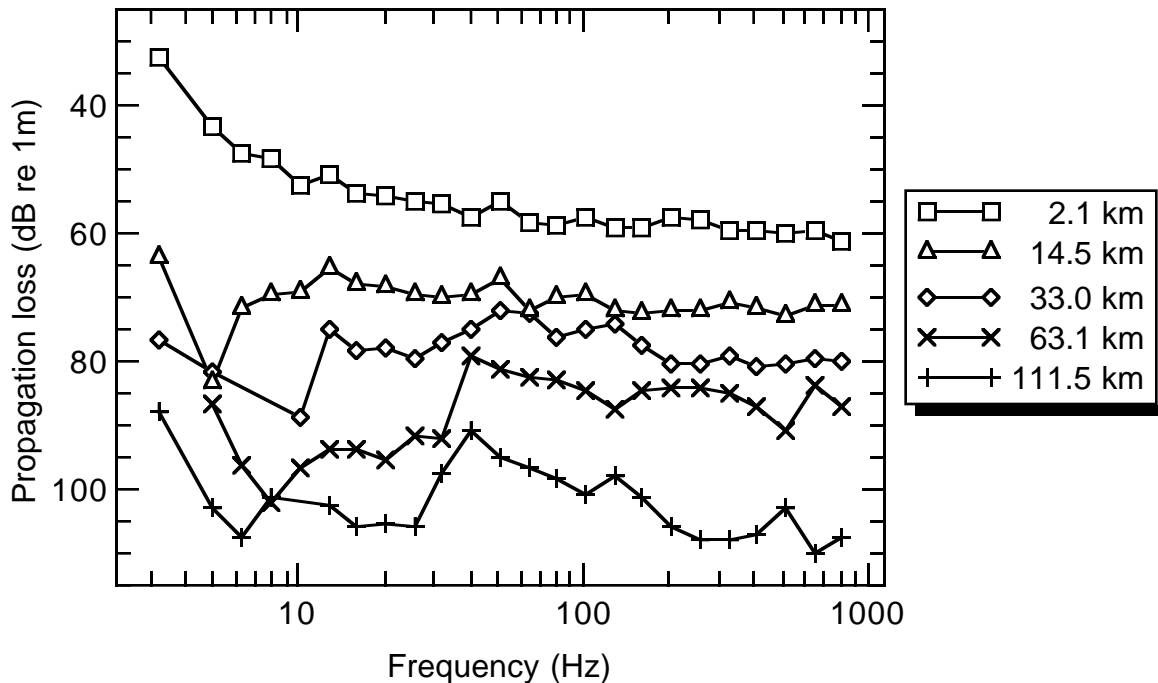


Fig. 4. Third-octave measurements of propagation loss to the deepest hydrophone (75.6 m) versus frequency for various ranges over the smooth seabed.

2.2.1. Propagation loss for a hydrophone depth of 75.6 m

As for our analysis of track SS, we plot frequency-averaged propagation loss as a function of range for track RS. These results are shown in Fig. 6. In this case, we also remove spherical spreading from the propagation loss (subtracted $20 \text{ Log}_{10}[\text{range in m}]$), so that the relationship between propagation loss and water depth might become more evident. Negative losses indicate less loss (i.e. better propagation) than a spherical spreading law and one metre reference range would produce.

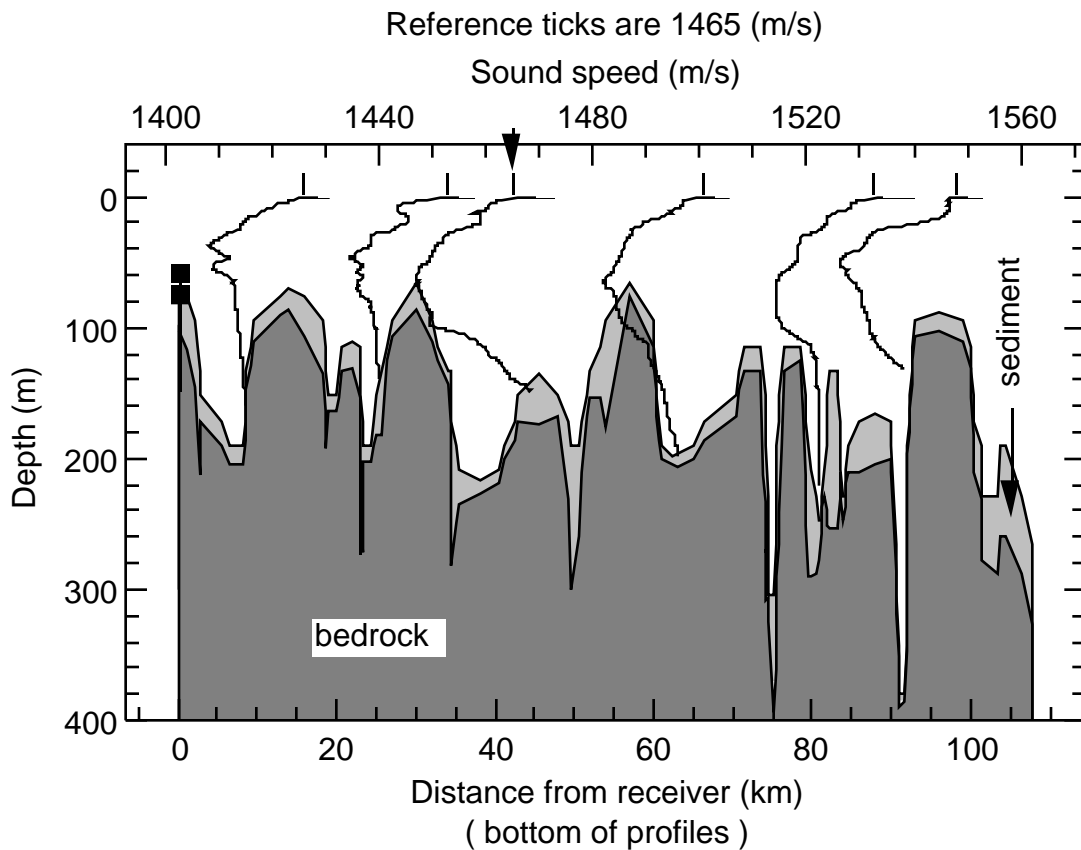


Fig. 5. Seabed depth and bedrock depth as a function of distance from the receiving hydrophone array for the rough seabed. The two hydrophones used in this study are shown as ■ symbols. Sound-speed data from XBTs are also shown, with their distance from the array indicated by the location of their bottom data points. A reference tick is drawn at the top of each sound-speed trace to indicate 1470 m/s.

Comparing the propagation loss and seabed depth curves in Fig. 6, we conclude that there is an observable correlation between the variation in propagation loss and the water depth. Minima in propagation loss tend to correspond to depth minima and so on. This relation is less evident at the long-range end of the track, where the propagation loss is higher. A mathematical analysis of the correlation coefficient yielded a value of 0.4 (between 0.23 and 0.55 with 95% confidence). The correlation coefficient r was calculated by the formula [CRC Standard Mathematical Tables, 1978]:

$$r = \frac{n\sum x_i y_i - (\sum x_i)(\sum y_i)}{\sqrt{\left[n\sum x_i^2 - (\sum x_i)^2 \right] \left[n\sum y_i^2 - (\sum y_i)^2 \right]}} \quad (1)$$

where there are $n = 108$ (x,y) pairs, x is the frequency-averaged propagation loss (with spherical spreading removed) in dB re 1m, y is the depth in metres, and the pairs lie at every kilometre from 1 to 108 km. The propagation loss and water depth were interpolated with respect to range in order to give this uniform range spacing.

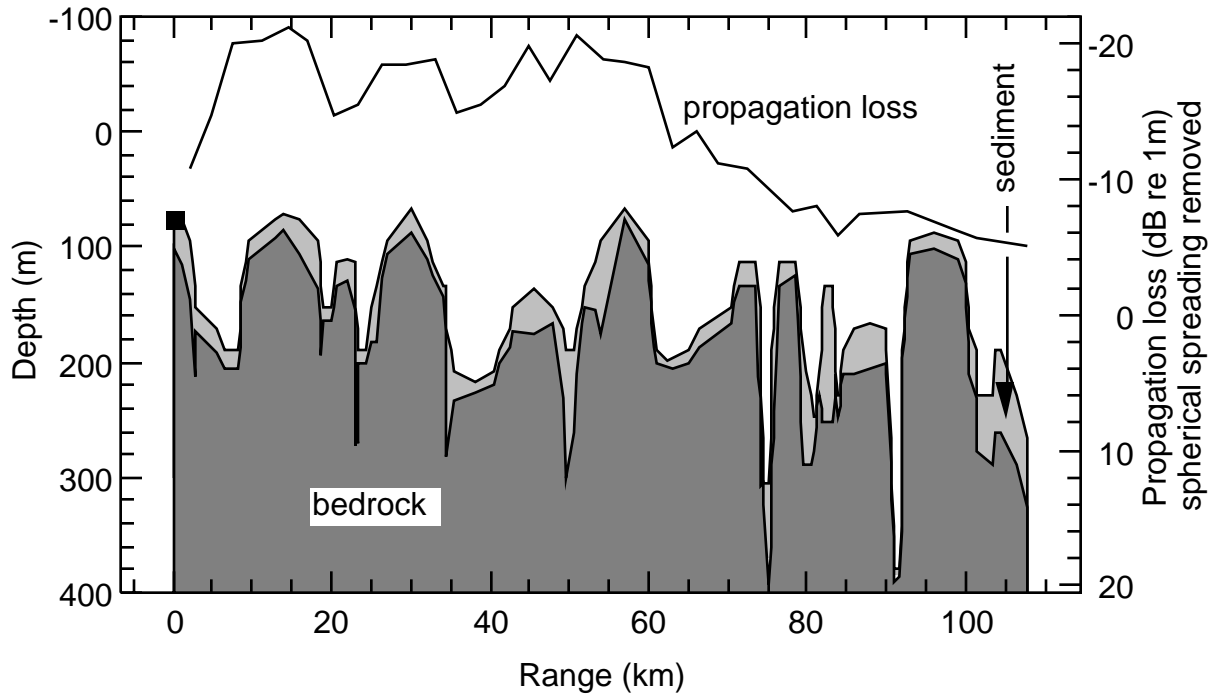


Fig. 6. Frequency-averaged experimental propagation loss (with spherical spreading removed) to the deepest hydrophone (75.6 m, marked with ■ symbol) as a function of range. Seabed depth and bedrock depth as a function of distance from the receiving hydrophone array for the rough seabed are also shown.

Sediment thickness appears to have little observable effect on the propagation loss for the case of the rough seabed. Two possible reasons for this are: 1) the small variation in sediment thickness, and 2) the small scale of variations in propagation loss due to sediment thickness effects, compared with those due to changes in water depth.

Propagation loss is plotted as a function of frequency in Fig. 7. Data are shown for ranges of 7.7, 14.5, 51.0, 78.1, and 101.4 km. We see a similar character in propagation loss-versus-frequency as for the smooth-seabed track (Fig. 4). That is: for short ranges, acoustic propagation loss generally increases with increasing frequency, but for long ranges, there is a maximum in the acoustic propagation loss near 10 Hz. For the rough seabed track, however, the low-frequency maximum in the acoustic propagation loss (apparent at longer ranges) is more pronounced (20 to 30 dB instead of 15 to 20 dB). The maxima are also at slightly higher frequencies: in the region of 4 to 20 Hz. At the two longest ranges (78.1 and 101.4 km) the acoustic propagation loss increases below about 90 Hz, but decreases again below 10-20 Hz. This behavior in loss is similar to the propagation loss measured over rocky seabeds with little sediment cover [Staal, Chapman and Zakarauskas, 1986].

As for the case of the smooth seabed, the propagation loss decreases at the very low frequencies, below about 10 Hz (if we ignore data for the two shortest ranges). This behavior is considered to provide evidence of compressional, shear or interface waves propagating in the bottom layers, since the water layer is too thin to carry such long wavelengths by itself. The modal cutoff is at approximately 10 Hz for the shallower portions of track RS [Akal and Jensen, 1986].

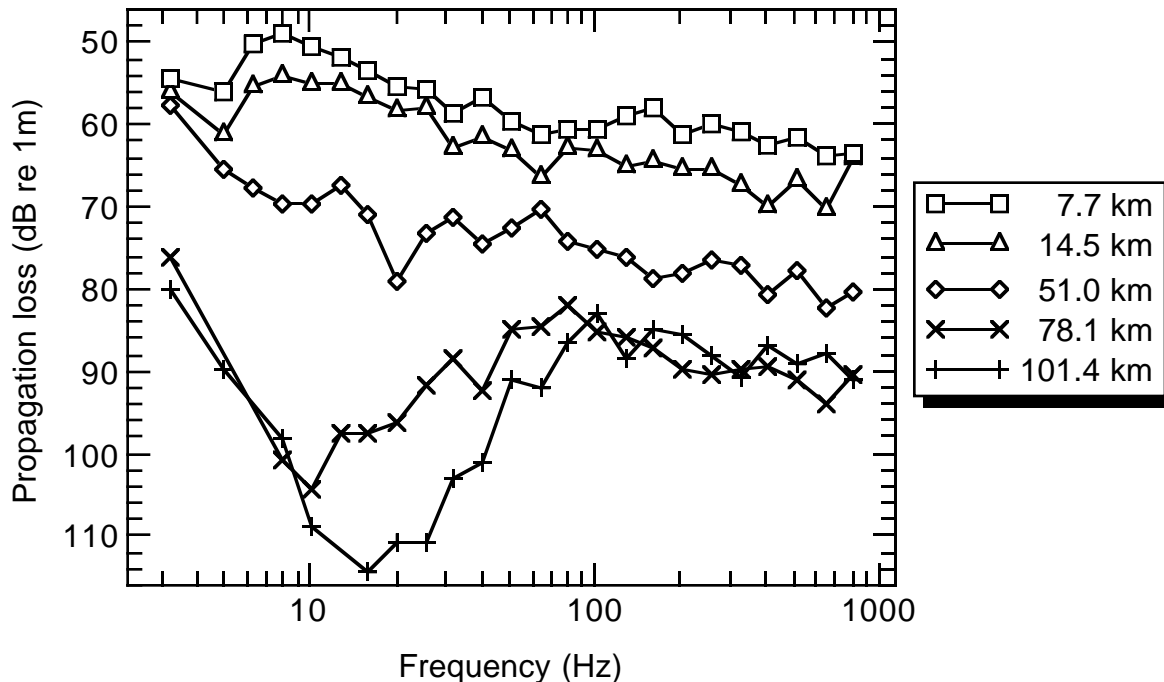


Fig. 7. Third-octave measurements of propagation loss to the deepest hydrophone (75.6 m) versus frequency for various ranges over the rough seabed.

2.2.2. Propagation loss for a hydrophone depth of 62.1 m

For track RS we also examined data from the hydrophone at 62.1 m depth. The propagation loss versus frequency data for the 62.1 m hydrophone present the same characteristics as those described previously for the 75.6 m hydrophone, and are therefore not shown here. Figure 8 shows frequency-averaged experimental propagation loss (with spherical spreading removed) as a function of range, for the hydrophone at 62.1 m depth (marked with ■ symbol). Seabed depth and bedrock depth as a function of distance from the receiving hydrophone array are also shown.

The variation in frequency-averaged propagation loss as a function of range appears to show a very slight correlation (correlation coefficient is only 0.1) with the water depth. This correlation is not as strong as for the deeper hydrophone. The weaker correlation for the 62.1 m depth hydrophone is probably explained by the presence of the sound channel. The shallower hydrophone is located nearer the axis of the sound channel and so receives significant energy arriving via paths which do not interact with the seabed.

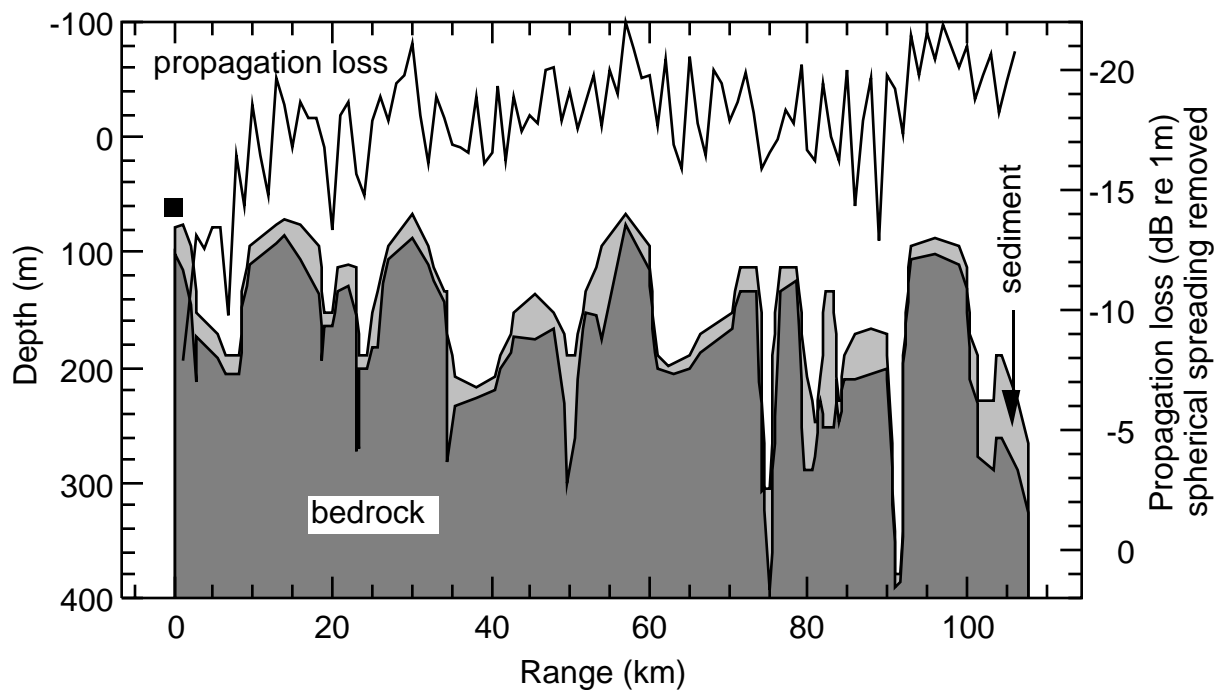


Fig. 8. Frequency-averaged experimental propagation loss (with spherical spreading removed) to the 62.1 m deep hydrophone (marked with ■ symbol) as a function of range. Seabed depth and bedrock depth as a function of distance from the receiving hydrophone array for the rough seabed are also shown.

2.3. COMPARISON OF LOSS FOR SMOOTH AND ROUGH SEABEDS

In general, the character of the propagation loss (expressed as a function of either range or frequency) is quite different for the two tracks, despite the fact that the same receiving hydrophones were used for both.

It is highly probable that the sediment types are similar for both tracks, since both are located in the same general region. Sediment thickness data for the smooth-seabed track are sparse, but indicate a significantly thicker deposit (on average) than for the rough-seabed track. Figure 9 compares propagation loss as a function of range for the two tracks at three frequencies, 25 Hz, 102 Hz, and 406 Hz. We see here that the propagation loss over the smooth seabed is nearly always higher (by 5 to 10 dB) than the loss over the rough seabed. This difference may be due to the fact that there is less acoustic interaction with the seabed for the case of the rough seabed; the acoustic energy is partly trapped in a sound channel.

Water depth seems to have a more significant effect on propagation loss than does sediment thickness. For propagation over the rough seabed we find a significant correlation (a correlation coefficient of 0.4) between fluctuations in propagation loss (less $20 \text{ Log}_{10}[\text{range in m}]$) and depth fluctuations. For the case of the smooth seabed, no significant correlation is observed simply because the water depth changed very little. That water depth should have a greater effect than sediment thickness is expected at higher frequencies (frequencies at which the sediment layer is at least several shear wavelengths thick) where the sound energy tends to travel more in the water than in the seabed [Akai and Jensen, 1986; Hughes, Ellis, and Staal, 1989]. For a typical sand shear speed $c_s = 170 \text{ m/s}$, the frequency at which the sand layer is three shear wavelengths thick is $f_{3s\lambda}$, where:

$$f_{3s\lambda} = \frac{3 c_s}{t_{sed}} = \frac{510}{t_{sed}} . \quad (2)$$

For the smooth seabed, $f_{3s\lambda} \approx 3.1 \text{ Hz}$, and for the rough seabed, $f_{3s\lambda} \approx 17 \text{ Hz}$. At frequencies below $f_{3s\lambda}$, one would expect the sediment thickness variations to significantly affect the propagation loss [Hughes, Ellis, and Staal, 1989]. For the rough-seabed propagation loss shown in Fig. 7, the low-frequency maximum (apparent at longer ranges) may be due to the apparently thin sediment below $f_{3s\lambda} \approx 17 \text{ Hz}$.

For both seabeds, we suspect that compressional, shear and/or interface waves propagating in the bottom layers are contributing to the received sound energy. The reduction in propagation loss at very low frequencies ($f < 5 \text{ Hz}$) seems indicative of this contribution [Akai and Jensen, 1986]. Since these frequencies are below the predicted modal cutoff frequency for the shallow water waveguide, we would expect that the sound must not be propagating in the water channel. For both the smooth-seabed track and the shallow regions of the rough-seabed track, the modal cutoff frequency is about 10 Hz. Note, however, that the deeper portions of the rough-seabed track will support water-borne acoustic modes down to about 5 Hz.

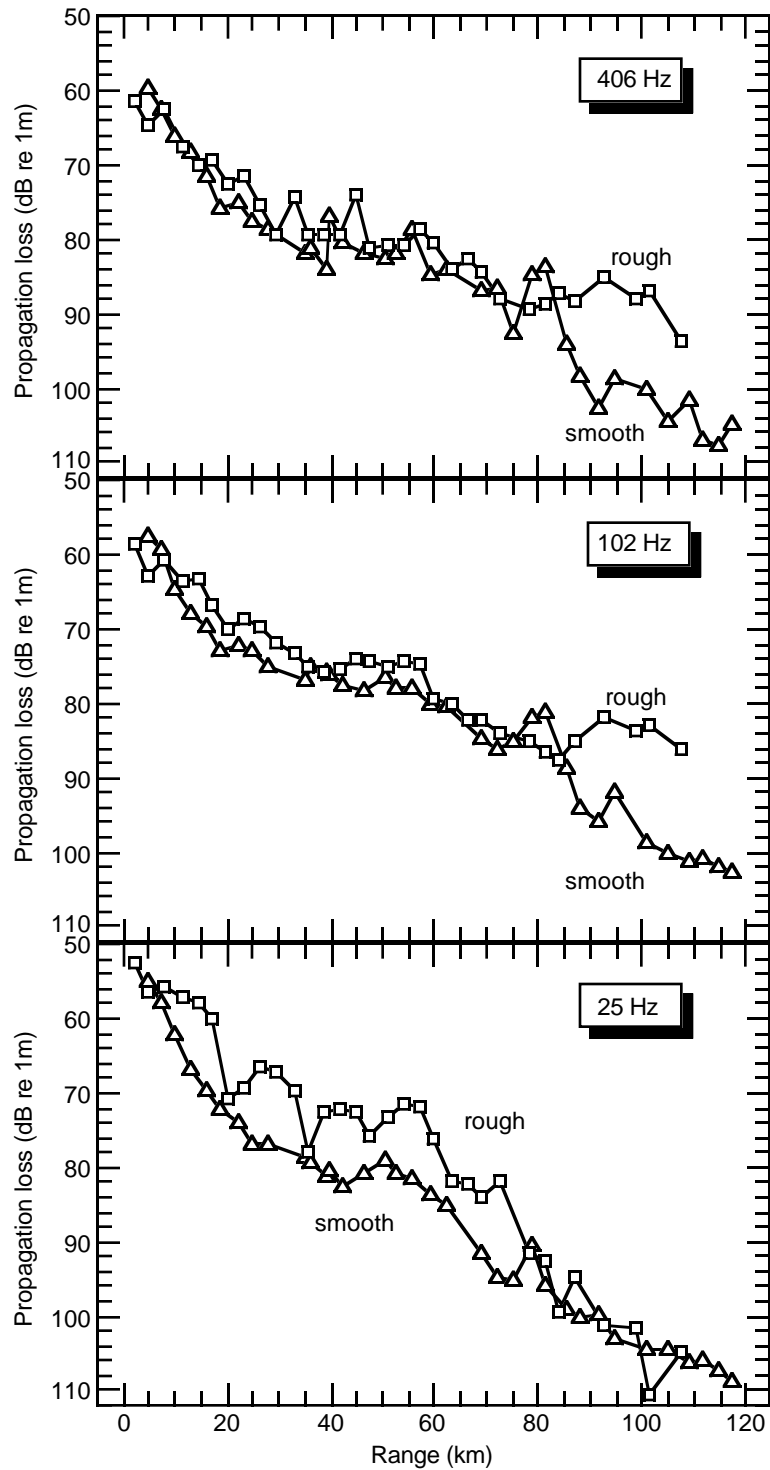


Fig. 9. Comparison of experimental propagation loss versus range for the rough and smooth seabeds. This comparison is shown at three frequencies: 25 Hz, 102 Hz and 406 Hz.

3. MODELLING AND COMPARISON

By modelling the propagation loss conditions for these environments we seek a better understanding of the measured propagation loss and the correlation between the variations in propagation loss and water depth. We also wish to determine if the contributions of shear waves in the seabed need to be considered in order to successfully model propagation loss over the smooth and rough seabeds.

3.1. SMOOTH SEABED

3.1.1. PROLOS

PROLOS is a DREA normal mode program [Ellis, 1985] that uses the adiabatic approximation (no acoustic energy transferred between modes) [Pierce, 1965] to include range dependence. This model assumes a slow adaptation of the modes to the water depth without coupling between the modes. No energy is transferred between modes due to the changes of water depth, sound-speed profile or seabed roughness along the track. PROLOS calculates acoustic propagation losses due to geometrical spreading, and absorption in both the sea water and the seabed. The major shortcoming of this program is that it does not consider shear waves.

As input for PROLOS, we need the water depth, the sound-speed profiles along the track, the acoustic frequency, and a description of the acoustic properties of each significant seabed layer. There are seven sound-speed profiles along track SS (Fig. 2), but the water depth is defined at eleven range points. At each of these eleven ranges, we use the nearest available sound-speed profile to describe the environment. In general, there is a very slight sound channel about 50 m depth but an overall downward-refracting condition. The PROLOS input parameters used are given in Table I.

Table I. Water depth, sediment thickness, and sound-speed profiles input to PROLOS for the case of propagation over the smooth seabed.

Range (km)	Water depth (m)	Sediment thickness (m)	Sound-speed profile #
0	76	28	1
6.5	95	13	1
13	70	24.5	1
24	68	44	2
31.5	64	99.1	2
39.9	59	139	3
60	59	165	4
79	64	165	5
93	64.7	161	6
99	64	160	6
117	60	148	7

"Sediment thickness" is the thickness of the upper layer of sand sediment (see Fig. 2). The sediment is assumed to cover an "infinite" layer of bedrock, modelled by a 300 m thick layer in PROLOS. The water depth along each track was obtained from the depth contours on a surficial geology map of the Scotian Shelf (published by the Canadian Hydrographic Service). The thickness of the upper layer of sediment was interpolated from a sediment-thickness overlay for the same map [King, Nadeau, Maass and King, 1985].

3.1.1.1. PROLOS with a two-layer seabed

The seabed is characterized by the parameters [based on Akal and Jensen, 1983 and Mitchel and Focke, 1983] given below in Table II.

Table II. Two-layer seabed parameters for PROLOS.

Parameter	Sediment	Rock
Thickness (m)	(variable) ²	300
Density (g/cm ³)	1.8	2.1
Sound speed (m/s)	1700	2000
Attenuation (dB/m/kHz)	0.25	0.10

We begin the modelling study with a simple approximation for the seabed. We assume a homogeneous sand layer of variable thickness over thick bedrock, and we assign typical values to the seabed parameters for these types of sediments. Propagation loss is modelled at the discrete frequencies of 40 Hz, 102 Hz, and 406 Hz. Since one-third octave averaging is performed on the experimental data, they do not show the modal interference structure with range that the coherent discrete-frequency PROLOS model shows. However, PROLOS also provides an incoherent mode sum output that removes the modal interference structure. This incoherent output should therefore be in better agreement with the experimental data than the coherent output.

As shown in Fig. 10, there is reasonable agreement between the propagation loss data and the model for 102 Hz and 406 Hz, especially at short ranges. At 40 Hz for ranges beyond 39 km, the modelled data can differ by more than 10 dB from the experimental data. At shorter ranges (less than 39 km), we get better agreement. This discontinuity in propagation loss at 39 km is due to the fact that two portions of track SS were made during separate disjoint time periods. As shown in Fig. 11, the first part of the track was obtained while the ship was traveling away from the Hydra array, while for the second part of the track, the ship was travelling toward the array. We also see another abrupt change in the propagation loss, this one for all frequencies, at a range of 80 km. The wideband pressure-versus-time signals recorded from the hydrophones during the experiments also show this change, indicating that the change is not an artifact introduced by the 1/3 octave-band propagation-loss analysis. There is probably an environmental explanation for this second anomaly in the received signal level at 80 km, but so far we have not been able to model the phenomenon successfully.

² Determined from Table I.

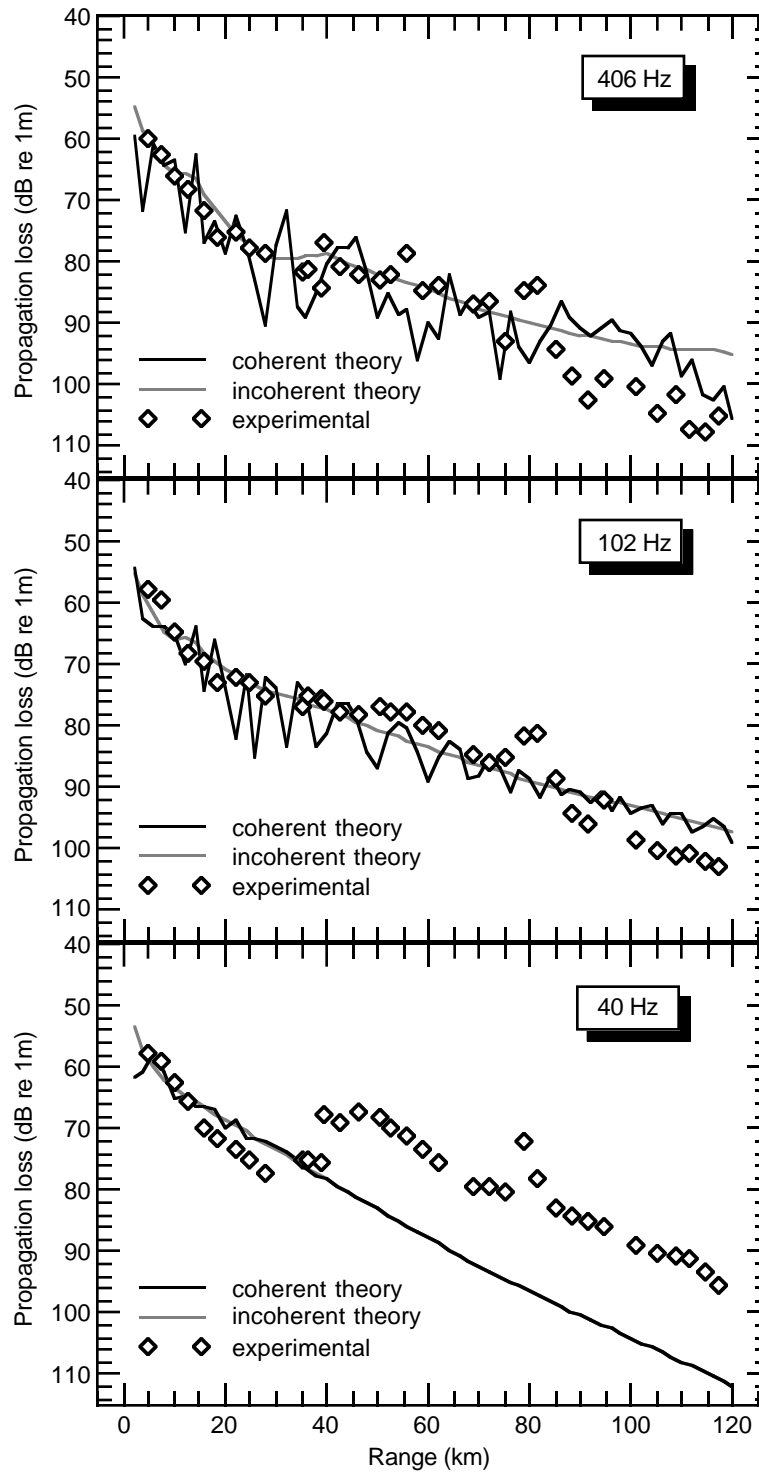


Fig. 10. Comparison at 40 Hz, 102 Hz and 406 Hz of experimental and theoretical propagation loss to the deepest hydrophone (75.6 m) versus range over the smooth seabed. The model used is PROLOS with a two-layer seabed, and the results for both coherent and incoherent mode addition are shown.

In order to explain the increase in propagation loss at long ranges, it might be appropriate to try different assumptions about the seabed. We therefore try a three-layer seabed model.

3.1.1.2. PROLOS with a three-layer seabed

We assume that the superficial sand layer model is actually two different overlying sand layers. The model for the bedrock sub-bottom layer is unchanged. The new parameters characterizing the seabed layers are as shown in Table III.

Table III. Three-layer seabed parameters for PROLOS.

Parameter	Sediment 1	Sediment 2	Rock
Thickness (m)	2	(variable) ³	300
Density (g/cm ³)	1.9	2.0	2.2
Sound speed (m/s)	1700	1800	2000
Attenuation (dB/m/kHz)	0.50	0.25	0.10

The Scotian Shelf is similar in many ways (including the sediment types) to the UK continental shelf. DREA's propagation loss data for the UK continental shelf have shown better agreement between experimental results and the PROLOS model when two sand layers are used instead of one [Ellis and Chapman, 1984]. A slightly reduced compressional speed and a higher attenuation coefficient for the upper layer are assumed. These two layers approximate the positive sound-speed gradient and the negative attenuation gradient that we usually find in sand [Ellis and Chapman, 1984]. The positive results of [Ellis and Chapman, 1984] give us confidence in the use of two separate sand layers, and lead us to try a similar model here.

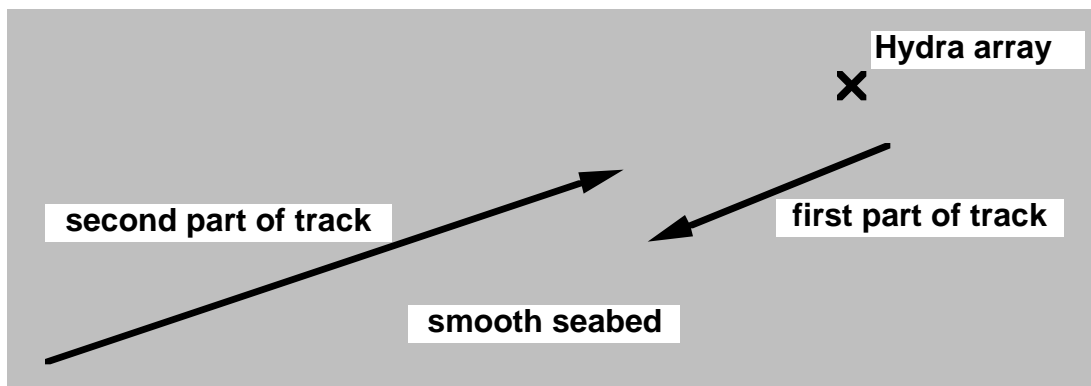


Fig. 11. Approximate map of the two parts of track SS over the smooth seabed relative to the Hydra array.

³ Determined from Table I.

The depth of penetration in the seabed is proportional to the wavelength. At high frequency (and short wavelength), therefore, most of the sound absorption by the seabed occurs in the top few metres of sand. The two metre-thick sand layer on top of the second sand and rock layers has a higher absorption coefficient than the second sand layer. The three layer bottom model should thus increase the propagation loss at high frequencies and improve the agreement between the modelled propagation loss and the experimental propagation loss. At low frequencies, the absorption takes place over a larger range of depths in the seabed; the upper layer should not affect the modelled low-frequency losses very much.

Fig. 12 shows the resulting comparison of model results and experimental data where the three-layer bottom model is assumed. The use of a three-layer seabed model, instead of the two-layer model, does not actually change the results much at 40 Hz. At 102 Hz and 406 Hz, we gain better agreement between the modelled and experimental propagation loss at long range, but agreement is degraded for intermediate ranges (≈ 30 to 80 km).

3.1.3. Comparison between the experimental results (over the smooth seabed) and the modelled results

Comparing the modelled propagation loss using PROLOS (with either a two- or three-layer seabed) with the propagation loss data for track SS, we conclude that PROLOS is reasonably successful for a smooth sandy seabed. The discontinuity in the path of the ship (at 39 km) that affects the experimental data remains an anomaly, of course. The sharp peak that is observed at 80 km is neither explained nor modelled.

Use of PROLOS with a three-layer seabed does not significantly improve overall agreement between modelled propagation loss and experimental data compared to PROLOS with a two-layer seabed.

3.2. ROUGH SEABED

We know of no previous attempt to model the propagation loss over such a rough seabed as track RS. The existence of the sound channel might be expected to reduce the interaction between the acoustic energy and the seabed. Prior to our analysis, therefore, we expected that the presence of the sound channel over the seabed would yield propagation loss results, modelled using PROLOS, to be in rough agreement with experimental measurements. Before discussing the results from PROLOS, however, it is useful to first discuss the high-frequency acoustic propagation paths predicted by a ray trace model.

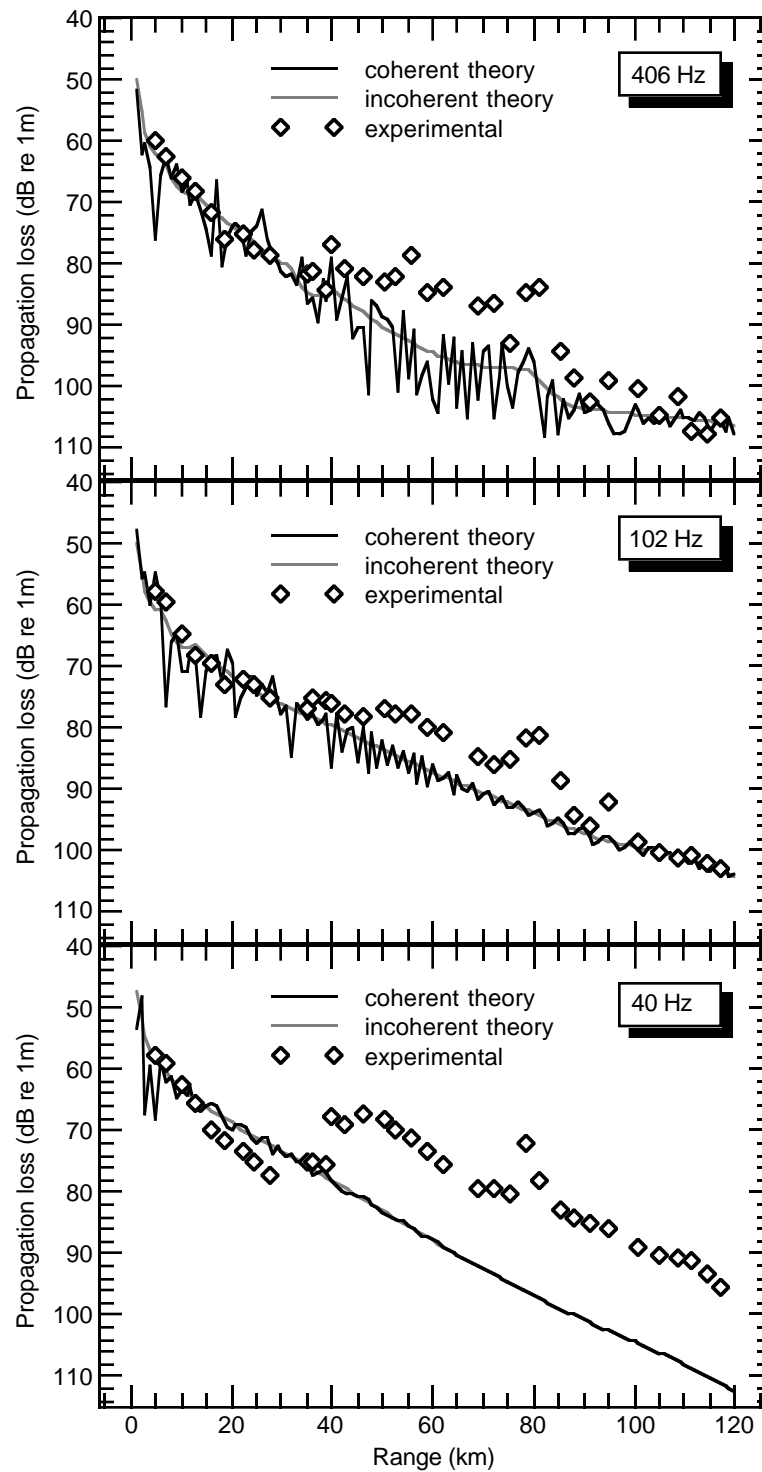


Fig. 12. Comparison at 40 Hz, 102 Hz and 406 Hz of experimental and theoretical propagation loss to the deepest hydrophone (75.6 m) versus range over the smooth seabed. The model used is PROLOS with a three-layer seabed, and the results for both coherent and incoherent mode addition are shown.

3.2.1. GRASS

GRASS is a range-dependent ray-trace model [Cornyn, 1973]. Simple ray theory may be inadequate to model shallow-water acoustic propagation loss, but it is nevertheless a good way to verify, by following the ray paths, where the acoustic energy goes.

We use the GRASS model for a receiver at the 75.6 m hydrophone depth, not far from the sound channel axis at around 60 m depth. Additional inputs to GRASS are: the water depth, the sound-speed profiles along the track, and a reflection loss table (reflection loss versus angle) to characterize the seabed. GRASS does not take account of sediment layers, but defines the seabed by reflection properties at the water-sediment interface.

For track RS, the water depth is defined at 145 different range points and there are six different sound-speed profiles along the track (Fig. 5). The reflection loss used is a simplification of data from Akal and Jensen (1983) as given in Table IV.

Table IV. Reflection loss versus grazing angle for sand.

Grazing angle (degrees)	Reflection loss (dB)
0.00	0.00
15.0	2.00
25.0	3.00
35.0	5.00
45.0	8.00
90.0	8.00

Figure 13 illustrates the ray paths for a near-horizontal ray (2.5 degrees) and a steeper-angle ray (7.5 degrees). (Keep in mind the 130 times vertical exaggeration in this figure). These paths are calculated for rays travelling upwards from the 75.6 m receiver position. The steeper ray propagates energy into the valleys but experiences many bottom bounces (particularly in shallower portions of the track), losing energy with each bottom interaction. Thus the steeper ray is of some importance at short range, but loses energy quickly with increasing range and is not an important contributor to energy at the receiver for longer ranges. The majority of the energy from long range arrives at the receiver via near-horizontal rays. Such rays interact infrequently with the seabed for the shallow portions of the track and are confined within the sound channel in deeper water. The interaction between the acoustic energy and the seabed is therefore limited, and this knowledge should help the understanding of such an environment.

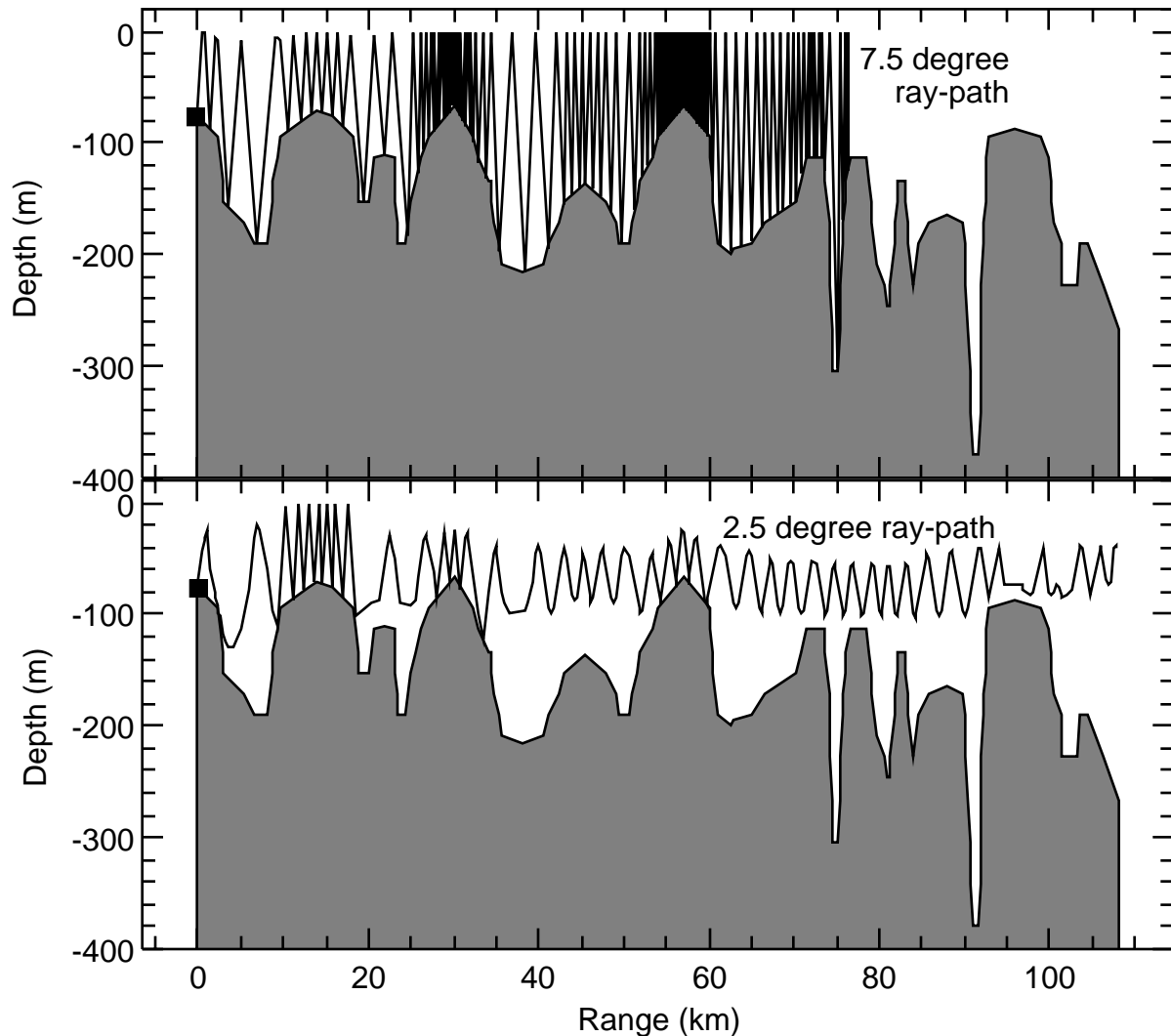


Fig. 13. Seabed depth as a function of distance from the receiving hydrophone array for the rough seabed. A 2.5 degree (off horizontal) ray-path and a 7.5 degree ray-path from the deepest hydrophone (75.6 m, marked with ■ symbol) are superimposed on these bathymetric plots.

3.2.2. PROLOS

Modelling propagation loss over a smooth seabed has shown us that PROLOS can give reasonable results for a slightly range-dependent environment (as shown in Section 3.1; also [Ellis and Chapman, 1980]). For the rough seabed, the slopes are steeper (up to about 5 degrees for the rough seabed, 0.22 degrees maximum for the smooth seabed), and the water depth varies between roughly 90 m and 210 m every few kilometres in range. The number and shape of propagating acoustic normal modes are dependent on the water depth and seabed acoustic characteristics [Urlick, 1983]. Since the water depth and seabed characteristics change repeatedly along track RS, the normal modes are expected to change (in number, shape and excitation) in a corresponding way. The adiabatic mode theory (that PROLOS uses) is

only valid for cases in which the modes change slowly with range [Pierce, 1983]. We therefore expected that PROLOS might not be able to model propagation loss as accurately for track RS as for track SS.

The propagation loss data for track RS are significantly different for the two hydrophone depths studied. We therefore use PROLOS (with a three-layer seabed) to model propagation loss for both of these depths. The environmental input for PROLOS is obtained as described in Section 2. The water depth and sediment thickness are estimated at 32 points along the track (see Table V), and six sound-speed profiles are available (see Fig. 5). As for the other cases modelled, the closest sound-speed profile is taken to describe each range point along the track.

3.2.2.1. PROLOS results for a hydrophone depth of 75.6 m (near the seabed)

For the 75.6 m hydrophone depth, we use the three-layer model of the seabed. Figure 14 shows the modelled propagation loss for the three layer seabed as a function of range for three frequencies: 25, 161, and 645 Hz. For all frequencies, it is possible to recognize in Fig. 14 some of the influence of the major extremes in water depth. Sediment thickness does not appear to have a noticeable effect on the modelled propagation loss. The predominant feature is the correlation between sound propagation loss and water depth.

We calculate the correlation coefficient between propagation loss and depth along track RS for the case of the modelled frequency-averaged propagation loss. The average used here is the arithmetic mean of the propagation loss in decibels for the 1/3 octave frequency bands centred on 25, 40, 64, 101, 128, 161, 256, 406, and 645 Hz. Spherical spreading is removed from the loss data to remove the general trend. Figure 15 shows these propagation loss data as a function of range from the hydrophone at 75.6 m depth. Seabed depth and bedrock depth as a function of distance from the receiving hydrophone array for the rough seabed are also shown. A correlation coefficient of 0.4 is observed for the experimental propagation loss data; for the model using PROLOS (with a three-layer seabed), we find a greater correlation coefficient: 0.8 (between 0.72 and 0.86 with 95% confidence).

In Fig. 14, the major difference between the experimental propagation loss results and the propagation loss as modelled by PROLOS with a three-layer seabed is the larger loss in the experimental data for 25 Hz beyond 75 km. A possible explanation for this discrepancy is a presumed change in the seabed properties for ranges of 75-108 km. The surficial geology map shows the presence of numerous V-shaped valleys (probably former river valleys) in the range interval 70-110 km. These valleys are steeper and deeper than those existing over the portions of the track between 0 and 70 km.

Table V. *Water depth, sediment thickness, and sound-speed profiles input to PROLOS for the case of propagation over the rough seabed.*

Range (km)	Water depth (m)	Sediment thickness (m)	Sound-speed profile #
0	76.0	40.0	1
8.1	190.0	15.0	1
9.2	114.0	15.0	1
9.6	95.0	15.0	1
13.9	70.3	15.0	1
18.3	95.0	40.0	2
20.1	152.0	12.0	2
22.0	110.2	20.0	2
24.4	190.0	12.0	2
26.3	114.0	12.0	2
30.0	66.5	20.0	2
34.4	152.0	70.0	2
38.1	216.6	10.0	3
42.9	152.0	20.0	3
45.5	135.4	39.0	3
50.6	190.0	110.0	3
57.0	66.5	10.0	4
63.0	195.7	10.0	4
70.3	152.0	15.0	4
71.3	114.0	20.0	4
75.1	304.0	20.0	5
78.5	114.0	10.0	5
81.1	247.0	10.0	5
83.1	133.0	120.0	5
84.1	228.0	20.0	5
87.9	165.3	40.0	5
91.1	380.0	40.0	6
95.9	87.4	15.0	6
98.9	95.0	15.0	6
101.5	228.0	50.0	6
104.5	190.0	70.0	6
107.9	266.0	60.0	6

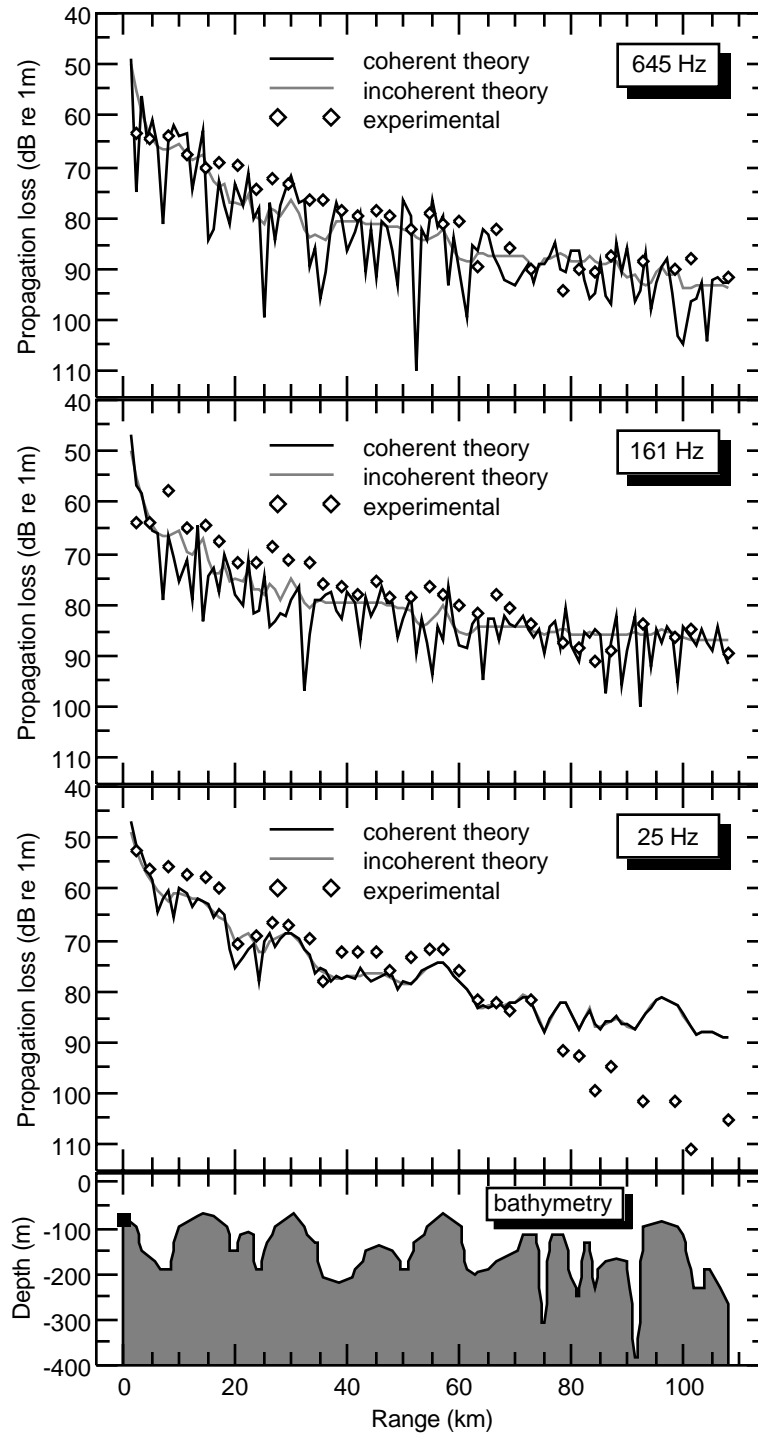


Fig. 14. Comparison of experimental and theoretical propagation loss to the deepest hydrophone (75.6 m, marked with ■ symbol) versus range over the rough seabed. This comparison is shown at three frequencies: 25 Hz, 161 Hz and 645 Hz. The model used is PROLOS with a three-layer seabed, and the results for both coherent and incoherent mode addition are shown. The water depth along track RS is shown at the bottom.

There are two possible seabed-property changes that could explain the higher experimental propagation losses at low frequencies for long range. First, the sediments could be more absorbent for the ranges beyond 70 km. Second, the rock seabed could be more exposed (thinner sediment and/or rock outcropping) at the longer ranges. The second possibility seems reasonable. We know that exposed rock gives us high losses at low frequencies [Hughes, Ellis, and Staal, 1989], and that the seabed near the long-range end of track RS is similar to (and near to) regions where high losses occur [Hughes, Ellis, and Staal, 1989].

3.2.2.2. PROLOS results for a hydrophone depth of 62.1 m (in the sound channel)

Fig. 16 shows experimental and modelled results for the 62.1 m receiver for track RS as a function of range for the same frequencies as used in Fig. 14. PROLOS with a three-layer seabed is the model used; all input parameters other than receiver depth are as for the 75.6 m receiver.

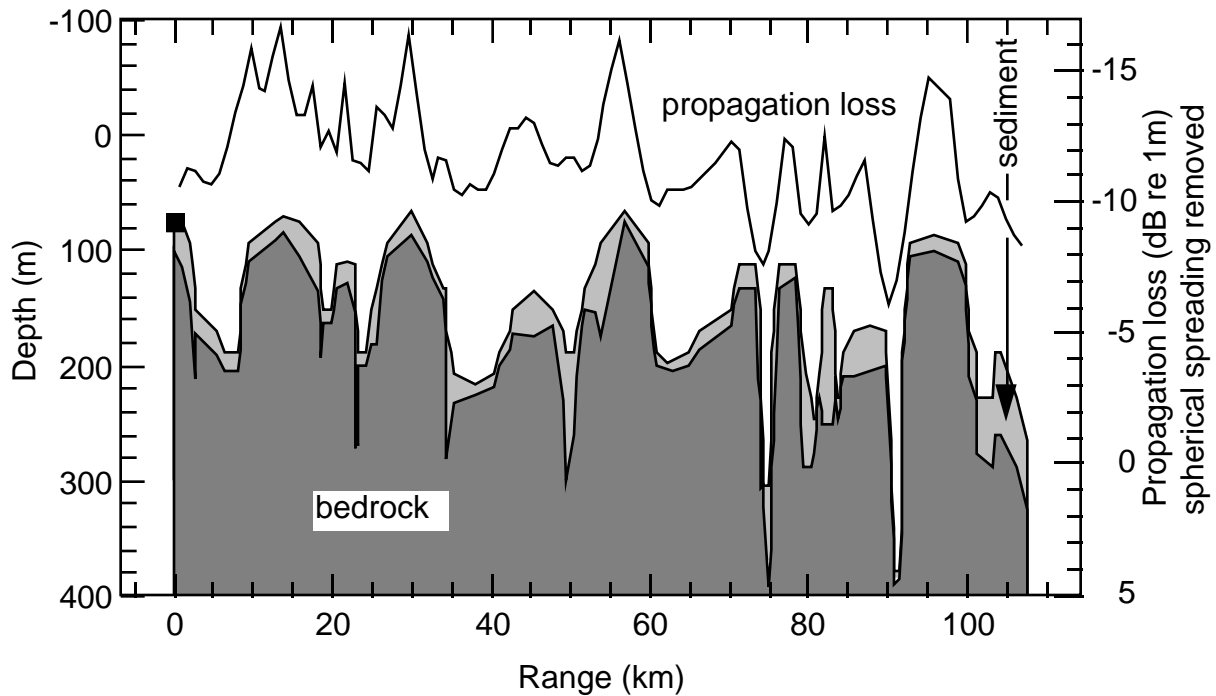


Fig. 15. Frequency-averaged theoretical propagation loss (with spherical spreading removed) to the deepest hydrophone (75.6 m, marked with ■ symbol) as a function of range. Seabed depth and bedrock depth as a function of distance from the receiving hydrophone array for the rough seabed are also shown.

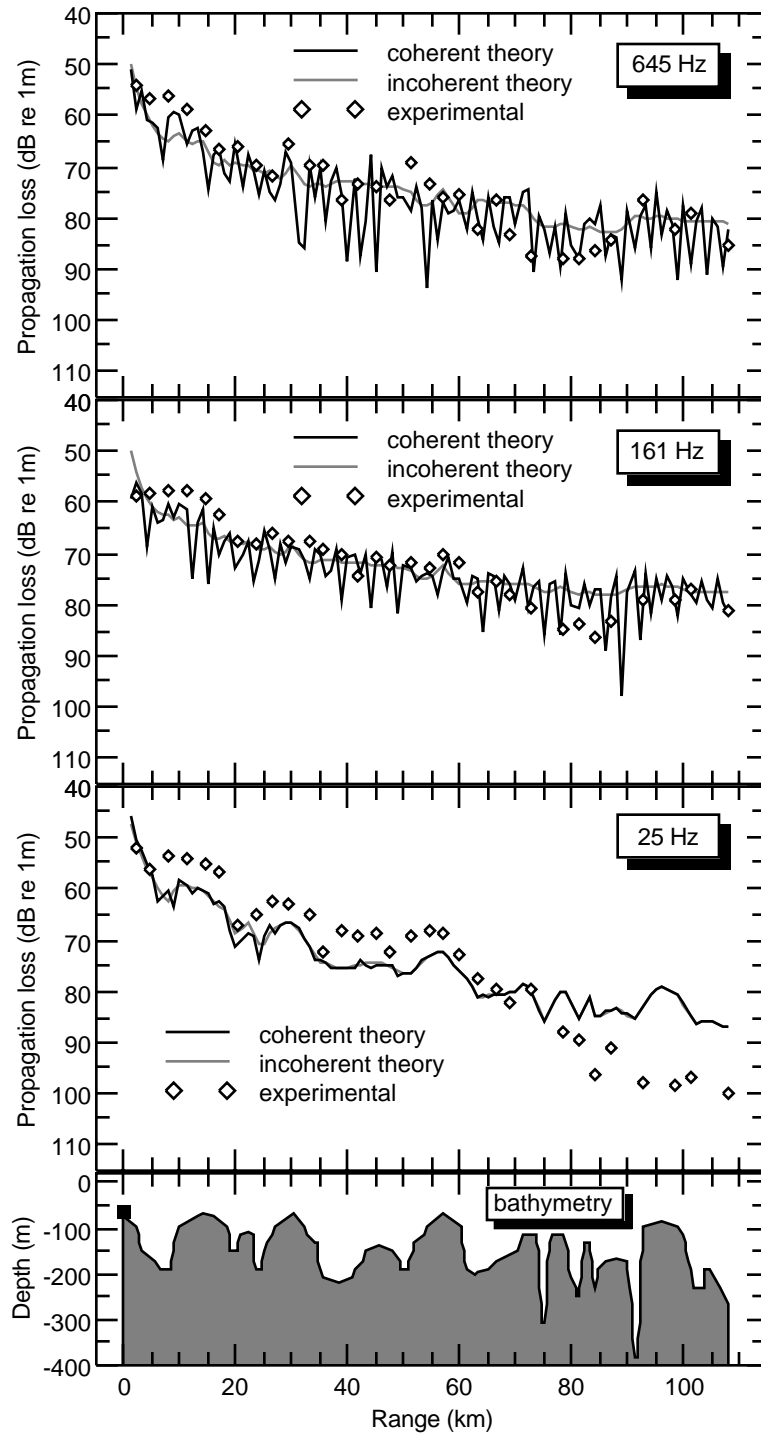


Fig. 16. Comparison of experimental and theoretical propagation loss to the 62.1 m deep hydrophone (marked with ■ symbol) versus range over the rough seabed. This comparison is shown at three frequencies: 25 Hz, 161 Hz and 645 Hz. The model used is PROLOS with a three-layer seabed, and the results for both coherent and incoherent mode addition are shown. The water depth along track RS is shown at the bottom.

The modelled propagation loss is in close agreement with the experimental propagation loss data. We see again a correlation in the model data between propagation loss and water depth, but the relation is not quite as evident as for the deeper hydrophone. The model results support our earlier explanation that there is significantly less bottom interaction for the sound propagation paths which reach the hydrophone at 62.1 m depth, compared with those paths which reach the receiver at 75.6 m.

3.2.3. Comparison between the experimental results (over the rough seabed) and the modelled results

PROLOS with a three-layer seabed is found to be adequate in modelling this example of long range sound propagation over a rough seabed. The results we obtain are close to the experimental propagation loss; this is partly due to the fortuitous existence of a sound channel which limits the degree of interaction of sound with the seabed. With a monotonically downward refracting sound velocity profile, one should not expect such close agreement between model and experiment.

It is speculated, however, that the use of another model may be necessary to explain losses due to shear waves or other similar phenomena, particularly for the low frequencies (below ≈ 100 Hz) at the long-range end of track RS. The necessity for incorporating shear waves in the model depends, of course, on the seabed layer types, and, in turn, on their capacity to support shear waves.

It seems that even if we simplify the seabed model to only two or three layers, we obtain reasonable agreement between modelled and experimental propagation loss. There is nevertheless a suggestion here that greater sophistication is needed in the model to account for the conditions which prevail at the longer ranges of track RS.

We see in both the experimental data and the model results a correlation between the propagation loss and the water depth. We observe this relation with PROLOS, even though PROLOS is not designed for the case where the seabed depth is changing rapidly with range.

We notice similar agreement between the experimental and the modelled results for the hydrophone at the seabed (75.6 m deep) and that near the centre of the sound channel (hydrophone at 62.1 m depth). It seems that the presence of a sound channel does not affect this agreement very much. We verify this conjecture by modelling the same environment with isospeed water, so as to avoid the effect of the sound channel. The resulting propagation loss information (shown as a function of range in Fig. 17 for frequencies of 25, 161, and 645 Hz) is quite similar to that for the original environment (Fig. 16) and shows essentially the same variability correlated with water depth.

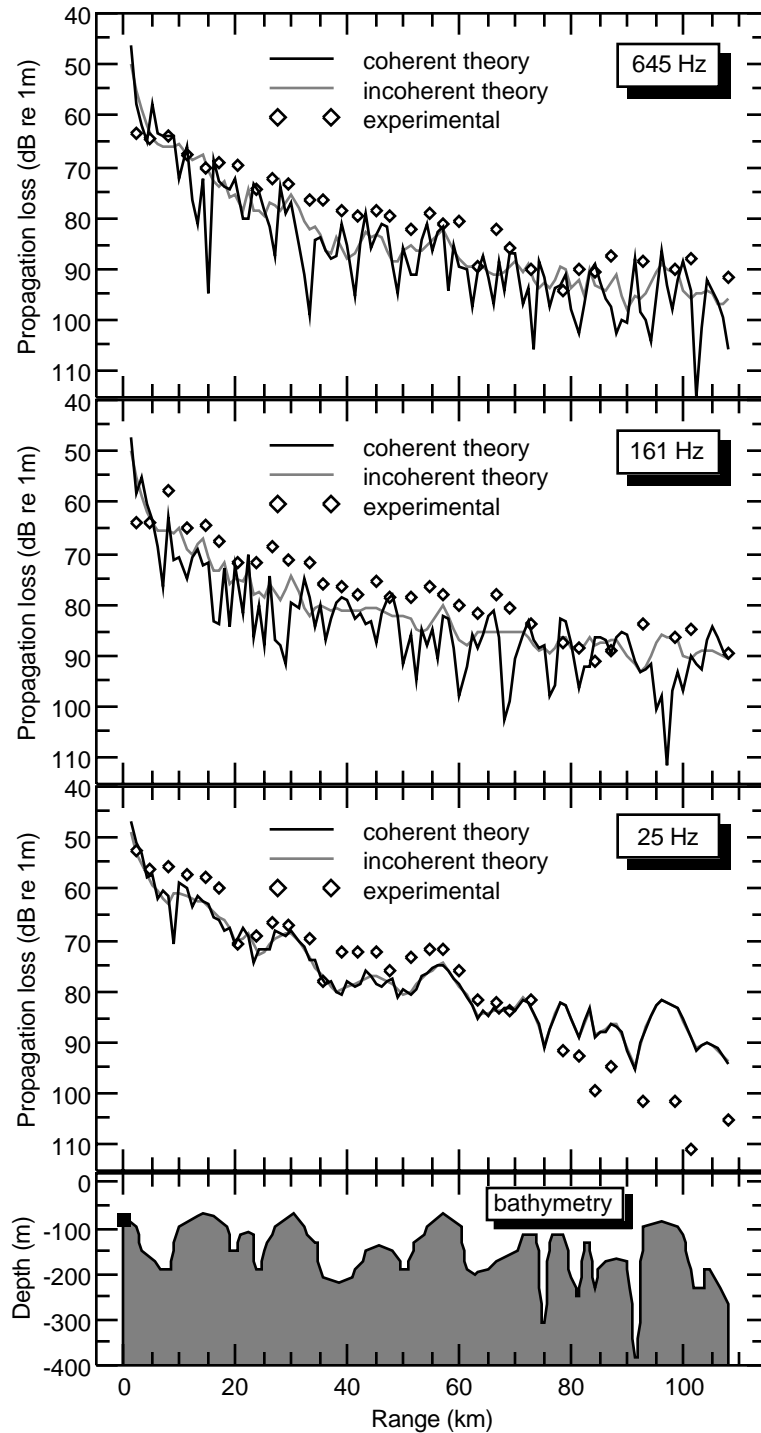


Fig. 17. Comparison of experimental and theoretical propagation loss to the deepest hydrophone (75.6 m, marked with ■ symbol) versus range over the rough seabed. This comparison is shown at three frequencies: 25 Hz, 161 Hz and 645 Hz. The model used is PROLOS with a three-layer seabed, and the results for both coherent and incoherent mode addition are shown. The water depth along track RS is shown at the bottom. This figure is identical to Fig. 14, except that the water layer was isospeed in the model.

4. CONCLUSIONS

This memorandum presents a study of acoustic propagation loss over two different but adjacent seabeds, one topographically smooth, the other rough. At-sea measurements show that the measured propagation losses are to some extent correlated with water-depth variations for the case of the rough seabed. In particular, the following points are noted.

- There is a significant correlation (coefficient ≈ 0.4) between acoustic propagation losses and water-depth variation over the rough seabed. (Because there is almost no depth variation there is no observable correlation between variations in depth and propagation loss for the case of the smooth seabed).
- The thickness of the uppermost seabed sediment layer does not appear to have a noticeable effect on propagation loss for either the smooth or the rough seabeds.
- The propagation loss over the smooth seabed is generally 5 to 10 dB higher than the loss over the rough seabed. This difference may be due to the fact that there is less overall acoustic interaction with the rough seabed. The presence of a sound channel in the deeper waters of the rough seabed track restricts the interaction of acoustic energy with the seabed to the shallower portions of the track.
- Low propagation losses are observed for tracks over both the smooth and rough seabeds at frequencies below about 5 Hz. This propagation feature is suggested to be evidence of compressional, shear or interface waves propagating in the bottom layers, since the water layer is too thin to carry such long wavelengths by itself (modal cutoff is approximately 10 Hz).

Modelled propagation-loss results from a ray-trace model (GRASS) and a normal-mode model (PROLOS) are compared with the at-sea measurements. The ray-trace model shows which acoustic transmission paths are most important while the normal-mode model is able to estimate the propagation-loss reasonably well over both the smooth and rough seabeds. In particular, the following points are to be noted with respect to modelling.

- The majority of the acoustic energy from long ranges arrives at the receiver by near-horizontal rays. Over the rough seabed, such rays interact with the seabed only for the shallower reaches of the track and are confined to a sound channel between peaks.
- For the rough seabed, the PROLOS normal-mode propagation-loss model yields a correlation (coefficient ≈ 0.8) between fluctuations in propagation loss and water depth. The modelled propagation loss matches the experimental results fairly well, even though PROLOS is not designed for the case where the seabed depth is changing rapidly with range.

- Including two sediment layers (sediment/sediment/rock) rather than one (sediment/rock) in the bottom model for PROLOS does not alter the apparent degree of agreement between the modelled and measured propagation losses.
- For the rough seabed, the major difference between the experimental propagation loss results and the propagation loss as modelled by PROLOS is the higher loss in the experimental data at low frequency (less than ≈ 100 Hz) for ranges greater than 75 km. It may be that the rock seabed at longer ranges is more exposed (thinner sediment and/or rock outcropping). Thinner sediment cover gives high losses at low frequencies in earlier studies, and the environment near the long-range end of the rough-seabed track is similar to (and near to) regions where high losses (thought to be due to thin sediment cover) occur.
- The sound channel observed over the deeper regions of the rough seabed track appears to have only a small effect on the propagation loss results.

In this memorandum, experimental and theoretical propagation loss have been compared in mostly qualitative terms rather than with quantitative statistics. There are several reasons for not using more quantitative terms: 1) the data presented here are a small sample that is not very significant statistically; 2) for a fair quantitative comparison, the theoretical data should be calculated for one-third octave averages to precisely match the experimental analysis; 3) the comparison error surface is at least four dimensional (location, range, frequency) and will likely require a multi-dimensional quantitative comparison; and 4) the emphasis in this memorandum is to understand the physical mechanisms in sound propagation rather than to fine-tune a predictive model. However, in future work, it is hoped that by considering a wider range of propagation loss cases and including models matched to our experimental methods, it will be possible to quantitatively define our acoustic propagation prediction capabilities.

It is concluded that the presence of a topographically rough seabed need not necessarily deter one from using a shallow water propagation loss model intended only for slow topographic variations. In the examples studied here, the PROLOS model works as well for propagation over a rough bottom as it does for propagation over a smooth seabed, for frequencies above 40 Hz.

REFERENCES

- Akal, T., and Jensen, F. B. (1983). "Effects of the sea-bed on acoustic propagation," *in: Acoustics and the Sea-Bed*, edited by N.G. Pace (Bath University Press, Bath, UK), pp. 225-232.
- Akal, T., and Jensen, F. B. (1986). "Ocean seismo-acoustic propagation," *in: Progress in Underwater Acoustics*, edited by H. M. Merklinger (Plenum Press, New York), pp. 493-500.
- Berkson, J. M., and Matthews, J. E. (1983). "Statistical properties of sea-floor roughness," *in: Acoustics and the Sea-Bed*, edited by N.G. Pace (Bath University Press, Bath, UK), pp. 215-223.
- Chapman, D. M. F. (1980). "The directional nature of the attenuation of sound due to scattering at a rough ocean surface," *J. Acoust. Soc. Am.* **68**, 1475-1481.
- Cornyn, J. J. (1973). "A digital-computer ray-tracing and transmission-loss-prediction system: Volume 1 - Overall description," NRL Report 7621.
- CRC Standard Mathematical Tables. (1978). CRC Press, Boca Raton, Florida. Probability and Statistics, p. 510.
- Ellis, D. D., and Chapman, D. M. F. (1980). "Propagation loss modelling on the Scotian Shelf: comparison of model predictions with measurements," *in: Bottom Interacting Ocean Acoustics*, edited by W.A. Kuperman and F.B. Jensen (Plenum Press, New York, N.Y.), pp. 541-555.
- Ellis, D. D., and Chapman, D. M. F. (1984). "Modelling of shear-wave related acoustic propagation on the UK Continental Shelf," DREA Technical Memorandum **84/P**.
- Ellis, D. D. (1985). "A two ended shooting technique for calculating normal modes in underwater acoustic propagation," DREA Report **85/105**.
- Hughes, R. C. (1981). "Underwater explosives: scaling of source spectra", *in: Underwater Acoustics and Signal Processing*, pp. 87-91, L. Bjørnø, ed., D. Reidel Publishing Company.
- Hughes, S. J., Ellis, D. D., and Staal, P. R. (1989). "Low-frequency acoustic propagation loss in shallow water over a hard-rock seabed covered by a thin layer of sediment," in preparation for JASA.
- Jensen, F. B., and Schmidt, H. (1986). "Spectral decomposition of PE fields in a wedge-shaped ocean," *in: Progress in Underwater Acoustics*, edited by H. M. Merklinger (Plenum Press, New York), pp. 557-564.
- King, E. L., Nadeau, O. C., Maass, O. C., and King, L. H. (1985). "Sediment thickness and seabed roughness studies - eastern Canadian continental shelf," DREA Contractor Report **85/407**.

- Mitchell, S. K., and Focke, P. C. (1983). "The role of the sea bottom attenuation profile in shallow water acoustic propagation," *J. Acoust. Soc. Am.* **73**, 465-474.
- Pierce, A. D. (1965). "Extension of the method of normal modes to sound propagation in an almost-stratified medium," *J. Acoust. Soc. Am.* **37**, 19-27.
- Pierce, A. D. (1983). "Augmented adiabatic mode theory for upslope propagation from a point source in variable-depth shallow water overlying a fluid bottom," *J. Acoust. Soc. Am.* **74**, 1837-1847.
- Staal, P. R., Hughes, R.C., and Olsen, J. H. (1981). "Modular digital hydrophone array," *in: Proceedings of IEEE Oceans '81*, pp. 518-521, Boston, Mass; re-issued as DREA Technical Memorandum **82/C**.
- Staal, P. R. (1987). "Use and evolution of a modular digital hydrophone array," *in: Proceedings of IEEE Oceans '87*, pp. 161-166; Halifax, N.S., Sep 28 to Oct 1, 1987.
- Staal, P. R. (1983). "Acoustic propagation measurements with a bottom mounted array," *in: Acoustics and the Sea-Bed*, edited by N.G. Pace (Bath University Press, Bath, UK), pp. 289-296.
- Staal, P.R., Chapman, D.M.F., and Zakarauskas, P. (1986). "The effect of variable roughness of a granite seabed on low-frequency shallow-water acoustic propagation," *in: Progress in Underwater Acoustics*, edited by H. M. Merklinger (Plenum Press, New York), pp. 485-492.
- Urick, R.J. (1983). *Principles of Underwater Sound* (McGraw-Hill, New York,1983), 3rd ed.

DOCUMENT CONTROL DATA		
(Security classification of title, body of abstract and indexing annotation must be entered when the overall document is classified)		
1. ORIGINATOR (the name and address of the organization preparing the document. Organizations for whom the document was prepared, e.g. Establishment sponsoring a contractor's report, or tasking agency, are entered in section 8.) <p style="text-align: center; font-size: large;">Defence Research Establishment Atlantic</p>	2. SECURITY CLASSIFICATION (overall security classification of the document including special warning terms if applicable). <p style="text-align: center; font-size: large;">Unclassified</p>	
3. TITLE (the complete document title as indicated on the title page. Its classification should be indicated by the appropriate abbreviation (S,C,R or U) in parentheses after the title). <p style="text-align: center; font-size: large;">Propagation-loss measurements and modelling for topographically smooth and rough seabeds.</p>		
4. AUTHORS (Last name, first name, middle initial. If military, show rank, e.g. Doe, Maj. John E.) <p style="text-align: center; font-size: large;">Staal, Philip R., and Desharnais, Francine</p>		
5. DATE OF PUBLICATION (month and year of publication of document) <p style="text-align: center; font-size: large;">June 1989</p>	6a. NO OF PAGES (total containing information Include Annexes, Appendices, etc). <p style="text-align: center; font-size: large;">38</p>	6b. NO. OF REFS (total cited in document) <p style="text-align: center; font-size: large;">21</p>
6. DESCRIPTIVE NOTES (the category of the document, e.g. technical report, technical note or memorandum. If appropriate, enter the type of report, e.g. interim, progress, summary, annual or final. Give the inclusive dates when a specific reporting period is covered). <p style="text-align: center; font-size: large;">DREA Technical Memorandum</p>		
8. SPONSORING ACTIVITY (the name of the department project office or laboratory sponsoring the research and development. Include the address). 		
9a. PROJECT OR GRANT NO. (if appropriate, the applicable research and development project or grant number under which the document was written. Please specify whether project or grant). <p style="text-align: center; font-size: large;">Project 1AD</p>	9b. CONTRACT NO. (if appropriate, the applicable number under which the document was written). 	
10a. ORIGINATOR'S DOCUMENT NUMBER (the official document number by which the document is identified by the originating activity. This number must be unique to this document). <p style="text-align: center; font-size: large;">DREA Technical Memorandum 89/214</p>	10b. OTHER DOCUMENT NOS. (Any other numbers which may be assigned this document either by the originator or by the sponsor). 	
11. DOCUMENT AVAILABILITY (any limitations on further dissemination of the document, other than those imposed by security classification) <input checked="" type="checkbox"/> Unlimited distribution <input type="checkbox"/> Distribution limited to defence departments and defence contractors; further distribution only as approved <input type="checkbox"/> Distribution limited to defence departments and Canadian defence contractors; further distribution only as approved <input type="checkbox"/> Distribution limited to government departments and agencies; further distribution only as approved <input type="checkbox"/> Distribution limited to defence departments; further distribution only as approved <input type="checkbox"/> Other (please specify):		
12. DOCUMENT ANNOUNCEMENT (any limitation to the bibliographic announcement of this document. This will normally correspond to the Document Availability (11). However, where further distribution (beyond the audience specified in 11) is possible, a wider announcement audience may be selected).		

13. **ABSTRACT** (a brief and factual summary of the document. It may also appear elsewhere in the body of the document itself. It is highly desirable that the abstract of classified documents be unclassified. Each paragraph of the abstract shall begin with an indication of the security classification of the information in the paragraph (unless the document itself is unclassified) represented as (S), (C), (R), or (U). It is not necessary to include here abstracts in both official languages unless the text is bilingual).

Acoustic propagation loss data were obtained along two radial tracks from a receiving array at a site on the Scotian Shelf. One track was over a smooth seabed and the other over a rough seabed. The features of the propagation loss data for the two seabed types have been analyzed and compared. At-sea measurements show that fluctuations in the propagation loss data are correlated with water-depth variations for the case of the rough seabed. Two different propagation-loss modelling programs are used in an attempt to explain the acoustic features observed over the two seabeds. The majority of the modelled results were obtained with PROLOS, a DREA-developed range-dependent normal-mode program. The results of a ray-trace propagation-loss model (GRASS) are also compared with the measured data. The ray-trace model provides insight on which acoustic transmission paths are most important, while PROLOS is able to model the propagation-loss over both the smooth and rough seabeds surprisingly well.

14. **KEYWORDS, DESCRIPTORS or IDENTIFIERS** (technically meaningful terms or short phrases that characterize a document and could be helpful in cataloguing the document. They should be selected so that no security classification is required. Identifiers, such as equipment model designation, trade name, military project code name, geographic location may also be included. If possible keywords should be selected from a published thesaurus. e.g. Thesaurus of Engineering and Scientific Terms (TEST) and that thesaurus-identified. If it not possible to select indexing terms which are Unclassified, the classification of each should be indicated as with the title).

underwater acoustics
shallow water
hydrophone arrays
underwater sound transmission
PROLOS
marine geophysics
continental shelves
submarine topographic features
surface roughness